KFKI-1982-47

M. MAKAI

HEXAN - A HEXAGONAL NODAL CODE FOR SOLVING THE DIFFUSION EQUATION

Hungarian Academy of Sciences

CENTRAL
RESEARCH
INSTITUTE FOR
PHYSICS

BUDAPEST

KFKI-1982-47

HEXAN - A HEXAGONAL NODAL CODE FOR SOLVING THE DIFFUSION EQUATION

M. MAKAI

Central Research Institute for Physics
H-1525 Budapest 114, P.O.B. 49, Hungary

HU ISSN 0368 5330
ISBN 963 371 933 X

ABSTRACT

This report provides the theory and user's manual of the HEXAN program, which is a nodal program for the solution of the few-group diffusion equation in hexagonal geometry. The theory based upon symmetry considerations, provides an analytical solution in a homogeneous node. WWER and HTGR test problem solutions are presented. The equivalence of the finite-difference scheme and the response matrix method is proven. The properties of a symmetric node's response matrix are investigated.

АННОТАЦИЯ

В отчете даны теория и инструкция для пользователей программы HEXAN, решающей малогрупповое уравнение диффузии в гексагональной геометрии. Теория основана на соображениях симметрии, дает аналитическое решение в гомогенном ноде. Тестовая задача по ВВЭР и по высокотемпературному реактору, охлажденному газом, изложена. Доказана эквивалентность конечно-разностной схемы и метода "response matrix". Исследуются свойства "response matrix" симметричного нода.

KIVONAT

A riport a HEXAN program elméletét és használatának módját ismerteti. A HEXAN program a kevéscsoport diffuziós egyenlet megoldását adja meg hatszöges geometriában. A szimmetria meggondolásokon alapuló elmélet analitikus megoldást szolgáltat egy homogén nódban. Közöljük VVER és magas hőmérsékletü gázhütéses reaktorokra vonatkozó tesztfeladatok megoldásait. Bebizonyitjuk a végesdifferencia séma és a response-matrix módszer ekvivalenciáját. Megvizsgáljuk szimmetrikus nódok válaszfüggvényeinek tulajdonságait.

1. INTRODUCTION

Coarse-mesh methods are indispensable instruments in reactor calculations. Following the development of power reactor types, the largest variety of methods has been elaborated for rectangular geometry whereas the appearance of HTGR, some fast reactors, as well as WWERs required coarse-mesh methods applicable to hexagonal or triangular geometry as well.

One aim of this report is to provide a detailed theory and description of the HEXAN code which is a nodal program for hexagonal geometry. Symmetry considerations lead to a method applicable to diverse geometries. By means of this method an analitical solution to the few-group diffusion equation is provided for hexagonal geometry with partial currents connecting the nodes. The resulting equations are of response matrix type what motivates studying the structure of the response matrices of symmetric nodes. We have shown that finite difference (FD) equations equivalent to the response matrix equations can always be found.

HEXAN solves the few-group diffusion equation in homogeneous nodes of hexagonal shape. The core must consist of hexagons and it must be represented by a 60 degree sector, on two boundaries of which either reflectional or rotational symmetry is assumed, while on the third boundary the common albedo boundary condition is allowed. The results are node-averaged group-fluxes as well as power densities and the eigenvalue k_{eff}.

The report starts with a short note on the diffusion equation and proceeds to a survey of the coarse-mesh methods, treating the nodal methods exhaustively (to the authors knowledge) though it was not our goal to enlist every publication in this field. The original paper was referred to in general, but it may happen that an idea is referred to through a comprehensive paper. An analytic solution for hexagonal goemetry is derived in Section 4. The inevitable group theoretical details are summarized in Appendix A. The acceleration methods used in HEXAN are given in Section 5, together with the description of the code. Section 6 gives the input output description. Test results are given in Section 7. As HEXAN is based on the response matrix (RM) method, the question of substituting the RM equations by a FD scheme is discussed in Appendix B.

Several subroutines of the HEXAN program were taken from the SIXTUS code, written by dr. J. Arkuszewski, and the author is deeply indebted to Eidg. Institut für Reaktorforschung (Würenlingen) for this courtesy.

Sections 5 and 6 may serve as user's manual.

2. WHAT IS THE DIFFUSION EQUATION?

Our method, as well as the program based on it, endavours to solve the diffusion equation, therefore it may be important for future users to know what is the diffusion equation good for?

We begin with answering the question from physical aspect: it can be found in standard textbooks [1], [2], [3] that the term "diffusion theory" is commonly used to refer to the mathematical description of transport of particles through a host medium when the Fick's law holds:

$$\underline{j}(\underline{x}) = -D\underline{\nabla}\varphi(\underline{x}) \quad , \tag{2.1}$$

where $\underline{j}$ is the particle current and φ is the particle density, and D is the diffusion coefficient. We assume that each quantity may depend on a parameter and, as this parameter is the energy of the neutron in reactor physics, this parameter is called energy and it may change only discreetly. Throughout the paper we neglect the time dependence. The notations are taken from reactor physics but it is not too difficult to find the corresponding notation for other branches of physics.

The diffusion equation, on the other hand, means an elliptical differential equation which can be cast into the following form:

$$\underline{\nabla}(f(\underline{x})\underline{\nabla}\varphi(\underline{x})) + g(\underline{x})\varphi(\underline{x}) = h(\underline{x}) \tag{2.2}$$

and the corresponding boundary condition is a linear expression of φ and the gradient

$$a\cdot\frac{\partial\varphi(\underline{x})}{\partial\underline{n}} + b\cdot\varphi(\underline{x}) = 0 \tag{2.3}$$

The presented method assumes that the region over which Eq.(2.2) is to be solved, is divided into subregions where f, g and h may be considered constant. The subregions are connected by the continuity of a linear expression of $\varphi(\underline{x})$ and $\partial\varphi/\partial\underline{n}$ (i.e. by the continuity of partial currents in reactor physics' terminology). This continuity is prescribed, however, only for the quantity integrated along the common boundary.

In Appendix B, it will be shown that the field of application of the diffusion equation is wider than it would follow from the above. The response matrix method can be shown to be transformable to a discretized diffusion equation if the node is symmetric. Using the prescriptions given in Appen-

dix B, one can determine, at least in principle, the constants that will give a solution equivalent to the response matrix method. In this way, however paradox it is, one can solve even some transport problems by diffusion theory expedient, thus applications to several branches of physics may be possible [4-8].

3. A SURVEY OF THE COARSE-MESH METHOD

Elaborate theoretical descriptions of reactor behaviour in use today involve group diffusion theory models [9], [10]. To reflect the basic spectral properties at least a few energy groups (2-20, depending on the reactor type) and several thousands, or sometimes even million spatial mesh points form the problem we have to cope with. The classical finite difference method (FDM) [11] is unable to cope with such a huge task; one promissing alternative to FDM is the coarse-mesh (CM) method.

CM methods [12], [13], [14] cover a wide range of approximations, from empirically corrected finite difference methods to sophisticated analytical methods. The rich variety of methods is usually classified as finite element methods (FEM) and nodal methods (NM). FEM has a firm theoretical basis [15], [16] so one can fix the error of the FEM beforehand and determine the order of approximation accordingly. Moreover the FEM uses a special technique [17] called sparse matrix technique. FEM as a separate category will not be discussed here [18]. A third category includes hybrid methods: there are possibilities of improving the traditional finite difference scheme so that it should give better results even for large meshes. This method is referred to as coarse-mesh finite difference (CMFD) method.

Fayers and Nash showed [19] that using a mesh as coarse as 4 points per a BWR assembly, the power can be predicted within 2.5 %. The relatively high accuracy is according to a compensating error due to spectral and mesh size effects. Modifying the fast group D in the reflector, to correct for transport effects, also leads to a systematic error compensation [20]. Borresen proposed a particularly simple coarse-mesh scheme [21], [22] which starts from point fluxes, determines the average flux so that the mesh size errors should be compensated. This method proved rather effective [23] in rectangular geometry and similar algortihms, with smaller-larger alterations, were elaborated for hexagonal geometry as well. The PYTHIA-4 code introduced a correction for transport effects [24], the BIPR-6 code combines the analytic solution with the finite difference scheme [25], the BORORO code can be used for even 4 energy-group problems [26]. (The extension of PRESTO to several groups is given in Ref. [27].) In the DEGEN code [28] a polynomial approximation is combined with the finite difference scheme, similar idea is given for rectangular geometry in Refs.[29], [30]. The combination of FDM with an analytical solution is in use for rectangular geometry as well [31], what is more, Wooley's algorithm [31] neglects the smaller eigenvalue [32].

First nodal methods were developed in relation to coupled core systems and coupled nodes in a single reactor [33-36]. The NM introduces average neutron fluxes directly from integral neutron diffusion or transport approximations, avoiding the use of numerical quadratures. A common form of the diffusion equation is

$$-\underline{\nabla} D_g \underline{\nabla} \Psi_g(\underline{x}) + \Sigma_g \Psi_g(\underline{x}) = \sum_{g'=1}^{G} \left(\frac{\nu\Sigma_{fg'}}{k_{eff}} \cdot \chi_g + \Sigma_{g'\to g}\right) \Psi_{g'}(\underline{x}) \quad , \qquad (3.1)$$

where - D_g is the diffusion constant in group g,
Σ_g the removal cross-section in group g,
$\Sigma_{g'\to g}$ the scattering cross-section ($g' \neq g$),
χ_g the fission yield in group g,
$\nu\Sigma_{fg}$ the neutron production cross-section in group g,
k_{eff} the effective multiplication factor or eigenvalue.

The rigorous nodal balance equation is obtained by integrating Eq.(3.1) over the volume of the node:

$$\sum_{i=1}^{n_F} \frac{F_i}{V} \tilde{J}_g^i + \Sigma_g \phi_g = \sum_{g'=1}^{G} \left(\frac{\nu\Sigma_{fg'}}{k_{eff}} \cdot \chi_g + \Sigma_{g'\to g}\right) \phi_{g'} \equiv \sum_{g'=1}^{G} W_{gg'} \phi_{g'} \quad , \qquad (3.2)$$

where n_F is the number of the node faces. The average flux is

$$\phi_g = \frac{1}{V} \int_V \Psi_g(\underline{x}) \, d\underline{x} \quad . \qquad (3.3)$$

The face-averaged net current is

$$\tilde{J}_g^i = -\frac{1}{F_i} \int_{F_i} D_g(\underline{x}) \underline{\nabla} \Psi_g(\underline{x}) \, d\underline{F}_i \quad . \qquad (3.4)$$

Without additional relationships between node-averaged fluxes and face-averaged currents Eq.(3.2) can not be solved. Another problem is the connection between adjacent nodes: the net current on the boundary must be the same when determined in adjacent nodes.

Early NMs used coupling by current [12]. Let $\tilde{J}_g^i$ be the normal component of the face-averaged net current at the boundary of the n-th and (n+1)-th node. Assuming that $\tilde{J}_g^i$ is linear in $\phi_g^{(n)}$ and $\phi_g^{(n+1)}$ - the upper index indicates the so far oppressed number of the node - we have:

$$\tilde{J}_g^i = p_g^{(n)} \phi_g^{(n)} + p_g^{(n+1)} \phi_g^{(n+1)} \quad . \qquad (3.5)$$

Expressing all the average currents by a formula analogous to Eq.(3.5) we can eliminate the net currents from Eq.(3.2) arriving at a system solvable for average fluxes. Although simulation codes [37], [38] based on the above idea have been used for practical calculations [39], [40], the obtained accuracy is lower that that of other NM.

Most modern nodal methods are based on coupling by partial currents [41], [42]: nodes are connected by incoming and outgoing currents. In diffusion

theory the partial currents are determined from the flux as

- the outgoing current $$J_g^i = \frac{1}{F_i}\int_{F_i} \frac{1}{4}[\Psi_g(\underline{x}) - 2D_g \frac{\partial \Psi_g}{\partial n_i}(\underline{x})]dF_i \qquad (3.6)$$

- the incoming current $$I_g^i = \frac{1}{F_i}\int_{F_i} \frac{1}{4}[\Psi_g(\underline{x}) + 2D_g \frac{\partial \Psi_g}{\partial n_i}(\underline{x})]dF_i \qquad (3.7)$$

and n_i is the outward normal to face i. Making use of the relation

$$\tilde{J}_g^i = J_g^i - I_g^i \qquad (3.8)$$

the nodal balance equation (3.2) is expressed by partial currents and average fluxes as

$$\sum_{i=1}^{n_F} \frac{F_i}{V} J_g^i = \sum_{i=1}^{n_F} \frac{F_i}{V} I_g^i + \sum_{g'=1}^{G} \left(\frac{\nu\Sigma_{fg'}}{k_{eff}} \cdot \chi_g + \Sigma_{g'\to g}\right)\phi_{g'} - \Sigma_g \phi_g \quad , \qquad (3.9)$$

and now an additional relationship is required between average fluxes and partial currents. This relation were known if we knew the flux inside the node, therefore we may seek an approximate analytical expression for the flux. Polynomial approximation is an obvious choice [42], the corresponding NM is called nodal expansion method (NEM). This idea has proved fertile in rectancular geometry since the coefficients of the polynomial can be expressed by face and volume averaged quantitites. Another important moment is the ingenious simplification achieved by introducing the cross-leakage [42]. To understand that new term, let us return to Eq.(3.1) and integrate it over the y and z variables:

$$-\frac{\partial}{\partial x} D_g \frac{\partial \Psi_{gx}}{\partial x} + \Sigma_g \Psi_{gx} = \sum_{g'=1}^{G} W_{gg'} \Psi_{g'x} + L_x(\underline{x}) \quad , \qquad (3.10)$$

where

$$L_x(\underline{x}) = \int_{-\ell_y/2}^{+\ell_y/2} dy \int_{-\ell_z/2}^{+\ell_z/2} dz \left(\frac{\partial}{\partial y} D_g \frac{\partial \Psi_g}{\partial y} + \frac{\partial}{\partial z} D_g \frac{\partial \Psi_g}{\partial z}\right) \qquad (3.11)$$

is called cross-leakage as it gives the sum of the y and z directed net leakage at point x (ℓ_y and ℓ_z are the thickness of the node in y and z directions, respectively). It is easy to see that $L_x(\underline{x})$ = const. allows only neutron paths such that a neutron having entered through a face normal to direction x, leaves through a face parallel to x. Perhaps even more important is that if $L_x(\underline{x})$ is not constant then both the incoming current and the net current vary along the node boundary. Unfortunately, the cross-leakage concept is not applicable to hexagonal or other "non-carthesian" geometry. It has been proven [43-48] that a second order polynomial approximation to the cross-leakage gives good results. The corresponding low ranking polynomial approximations to the flux are such that the involved coefficients need not be stored, we

can express them by means of face averaged quantities, e.g. a second order formula is

$$\Psi_{gx}(\underline{x}) = \phi_g + \frac{\Psi_{gx}(l_x/2)-\Psi_{gx}(-l_x/2)}{2}(2x-1) + \\ + (\phi_g - \frac{\Psi_{gx}(l_x/2)+\Psi_{gx}(-l_x/2)}{2})(6x(1-x)-1) \quad . \tag{3.12}$$

Expansion of the flux in terms of orthogonal polynomials (e.g. Legendre polynomials [44]) has also been realized in simulation codes. The adequacy of the second order cross-leakage has been persuasively demonstrated by the CIKADA response matrix code [49]. The polynomial method causes inconvenience in hexagonal geometry; thus in the HEXBU code [50] three independent variables were introduced in 2D. At present NEM seems to be also of restricted value in hexagonal geometry [51].

Considering the right hand side of Eq.(3.1) as a constant, the solution will consist of

$$e^{\pm\sqrt{(\Sigma_g/D_g)}x} \tag{3.13}$$

exponential functions, in a 1D homogeneous node. The exponentials are different in each group. Aoki and Tsuiki [52] approximated the flux by a linear combination of such exponentials. To improve that method Arkuszewski [53] expressed the coefficients of the linear combinations in an iterative way. Although when the right hand side of Eq.(3.1) involves an exponential, like Eq.(3.13), the particular solution is proportional to

$$(ax + b)e^{\pm\sqrt{(\Sigma_g/D_g)}x} \quad ;$$

thus after the n-th iteration the solution would be an n-th order polynomial multiplied with an exponential. A self-consistent method was obtained by approximating the RHS with a second order polynomial [48]. The source now consists of a sum of exponentials and polynomials and Gaussian collocation method is used to convert them into a second order polynomial [54].

The analytic solution to Eq.(3.1) is out of question in general. In the case of a homogeneous node, however, the solution can be given. First Eq.(3.1) is integrated over the transverse directions and the solution is expressed with the help of the eigenfunctions of the Laplace operator [32] (i.e. with the help of exponential functions exp(Bx)). The parameter B may have only G fix values (G = number of energy groups in Eq.(3.1)). Using that analytic solution either the coupling parameters (cf. Eq.(3.5)) can be determined [55] or the sought relationship between partial currents, or net currents, and node averaged fluxes can be determined. Taking the next direction we can resort to the cross-leakage again, in this case the solutions are expressed by the sum of the Laplace operator's eigenfunctions and a second order polynomial [47]. Repeating the above steps we get a solution restrained by the sole assumption of the cross-leakage. In the case of analytical solutions

even a constant cross-leakage is acceptable (as in the SEXI code [56]), but the TWO-STEP code [57] has markedly demonstrated the improvement due to a step-function cross-leakage. The algorithm is even more effective if only the nodes of inhomogeneous surrounding (reflector, interface between inhomogeneous regions) are treated in 2 energy groups, whereas the rest in one group only as in the CETRA code [58]. There is a possibility of solving Eq.(3.1) in the x-y directions simultaneously [59], [60]. The eigenfunctions now are $\exp(\underline{bx})$, $\underline{x} = (x,y)$ and $|\underline{b}|$ may have two values b_1 and b_2 ($<b_1$). The direction of the $\underline{b}$ vector may be chosen arbitrarily. Two choices are worth considering: the first one is $\arg(b) = n\pi/2$, $n = 0,1,2,3$; the second one is $\arg(b) = (n\frac{\pi}{2} + \frac{\pi}{4})$, $n=0,1,2,3$. The former is called plane-wave superposition (PWS), the latter nodally separable bucklings (NSB). NSB is used for the eigenvalue b_2, whereas PWS is used for the eigenvalue b_1. A third possibility is used in ANANAS [61]: the solution is expressed as linear combination of 8 exponentials. Each combination is invariant under the symmetry transformations of the node.

The solution may be attempted by determining the Green function of Eq.(3.1). The source is approximated by a polynomial, or trigonometric and exponential functions [62], [63]. A more consistent approach was proposed by Burns and Dorning [64], which introduces a multidimensional Green function and uses it to convert the diffusion equation into an integral equation for the within-node flux, in terms of the incoming partial currents on the node faces. Local polynomial expansions of the fluxes inside the node and the partial currents on the node faces are made. A local weighted residual or variational procedure generates equations relating the local expansion coefficients. The resulting equations are coupled to those for adjacent nodes by requiring that the partial currents across the node surfaces be continuous [46]. This method has successfully been used in thermal hydraulics as well [65].

At least two approaches exist for describing transport phenomena [66], [67]. In the first one the neutron flux distribution is the dependent variable. The equation for this flux expresses the neutron balance. This equation is approximated (or discretized) by a formula involving cross-sections and fluxes assigned to nodes. Finite difference equations are a typical example, but the mathematical structure of the equations allows one to define as nodal equations any set of linear equations of the form

$$(A_i + \sum_m C_{i,m})X_i - \sum_m C_{m,i} \cdot X_m = Q_i \quad , \qquad (3.14)$$

where $C_{i,m}$ - coupling coefficients between node i and m,
A_i - a parameter made up from cross-sections of node i,
Q_i - external sources.

The equations of the variational synthesis, the FEM [69], the CMFD method [21-26], the so-called nodal coupling method [70-72] can be cast into that form. Eq.(3.14) can be solved by standard numerical procedures which are

known stable. The same phenomena can also be described by means of transfer and scattering matrix methods originating from the theory of invariant imbedding. In these methods the average transmitted and reflected angular fluxes are the dependent variables. The classical form of the resulting transport equation is

$$\begin{bmatrix} J^{(1)} \\ J^{(2)} \\ \cdot \\ \cdot \\ \cdot \\ J^{(n_P)} \end{bmatrix} = \begin{bmatrix} R_1 & T_{21} \cdots\cdots & T_{n_P 1} \\ T_{12} & R_2 \cdots\cdots & T_{n_P 2} \\ \cdot & \cdot & \cdot \\ \cdot & \cdot & \cdot \\ \cdot & \cdot & \cdot \\ T_{1n_P} & T_{2n_P} \cdots\cdots & R_{n_P} \end{bmatrix} \begin{bmatrix} I^{(1)} \\ I^{(2)} \\ \cdot \\ \cdot \\ \cdot \\ I^{(n_P)} \end{bmatrix} , \qquad (3.15)$$

where $I^{(i)}$ denotes the number of entering neutrons at face i. $J^{(i)}$ denotes the number of neutrons exiting through the face i. R_k is the reflection coefficient of face k and T_{ij} is the transmission probability: entering at face i and leaving through face j. Eq.(3.15) is afflicted by instabilities, special care is needed when they are solved numerically [73]. In spite of this difficulty, response matrix methods are rather useful in reactor physics since:

A/ the method is flexible in practical applications as it may keep the internal structure of the node,

B/ response matrix functions are separately calculated (in advance),

C/ the equations are rigorous for any node size.

Response matrix method was first applied to cell calculation [74] and to diffusion theory [75]. Nodal programs employed [76] a somewhat altered form of the integral transport equation [42]:

$$J_g^{(k)} = \sum_{g'=1}^{G} P_{gg'}^{(k)} \phi_{g'} + \sum_{k'=1}^{n_P} P_g^{(k',k)} I_g^{(k')} \qquad , \qquad (3.16)$$

and the probabilities *P* were determined using a polynomial approximation to the flux. The method failed fulfilling the hopes [42] but in the CIKADA code the polynomial approximation to the flux and the response matrix method are successfully used [49]. In the SIMULATE code [77], however, a general response matrix algorithm is implemented and this code shows a remarkable flexibility as it includes, as special cases, the TRILUX invariant imbedding method [71], the FLARE method [70], the PRESTO method [21-23], the ROCS Taylor series expansion method [78], the CAROLE Fourier analysis method [78] and a transport Monte-Carlo method [79]. Almost every modern program uses an expression analogous to Eq.(3.16), and they differ in the determination of the coefficients *P*, see Ref. [9], [10], [26], [42], [23], [25], [56], [61], [80]. Some codes work with average fluxes and the response matrix equations are hidden in the derivation of the algorithm, see e.g. Ref. [47], [60]. In Appendix B we shall return to the response matrix method, and it will be

shown that Eq.(3.15) can always be converted intc nodal equations (3.14) if the node is symmetric.

Although some codes can cope with a heterogeneous node [42], [82] the need for a homogenization before the coarse-mesh calculation is still general. Traditionally this homogenization is separated from the coarse-mesh algorithm. Homogenization and the retaining of within-node flux distribution are open questions [80], [81], [82].

4. SYMMETRIES AND THE NODAL METHOD

Let us consider the G group diffusion equation in a homogeneous node:

$$-D_g\nabla^2\Psi_g(\underline{x}) + \Sigma_g\Psi_g(\underline{x}) = \sum_{g'=1}^{G}\left(\frac{\nu\Sigma_{fg'}}{k_{eff}}\chi_g + \Sigma_{g'\to g}\right)\Psi_{g'}(\underline{x}) \quad . \qquad (4.1)$$

In the present section an analytical solution to Eq.(4.1) is derived with the assumption that face-averaged partial currents are adequate for describing the boundary condition. The derivation can be used for any geometry, though here only the hexagonal geometry is considered.

It is well-known that eigenfunc ns of the Laplace operator are suitable for constructing an analytical solution [32]. First the eigenvalues are to be found from

$$(-D_g\lambda_k^2 + \Sigma_g)t_{kg} = \sum_{g'=1}^{G} W_{gg'}t_{kg'} \qquad (4.2)$$

where $\underline{t}_k = (t_{k1},\ldots,t_{kG})$ is the eigenvector. This problem means finding the eigenvalues and eigenvectors of a real G×G matrix. The problem had been solved, and several excellent techniques, available at program libraries [83], [84], support the numerical calculation. It is well-known that if G = 2, both eigenvalues are real, whereas in more than two groups complex conjugate eigenvalue pairs may occure. Altogether there are G different eigenvectors and eigenvalues. The solution is expressed by means of eigenfunctions of the Laplace operator as

$$\underline{\Psi}(\underline{x}) = \sum_{i=1}^{G}\int_{|\underline{\xi}|=1}\underline{t}_i c_i(\underline{\xi})e^{\lambda_i\underline{\xi}\underline{x}}d\underline{\xi} \equiv \sum_{i=1}^{G}\int_{|\underline{\xi}|=1}\underline{t}_i(\underline{\xi})e^{\lambda_i\underline{\xi}\underline{x}}d\underline{\xi} \quad , \qquad (4.3)$$

where $\underline{\Psi}(\underline{x}) \equiv (\Psi_1(\underline{x}),\ldots,\Psi_G(\underline{x}))$. $\underline{\Psi}(\underline{x})$ satisfies the DE (4.1) at each point inside the node as seen by substituting (4.3) into Eq.(4.1). The amplitude $c_i(\underline{\xi})$ has not been determined yet for it ensures the feasibility of arbitrary boundary condition specified along the boundary of the node. Eq.(4.3) is too complicated for practical purposes, therefore it will be simplified with the help of the symmetries of the node.

It is well-known that some geometrical transformations (e.g. rotations, reflections) leave the node invariant. In Appendix A it is shown that the eigenfunctions of these geometrical transformations may well be used in for-

ing the solution of Eq.(4.1). Let us return now to the basic concept of nodal methods, more precisely to Eq.(3.2) which is written now as

$$\sum_{i=1}^{6} J_g^i + \frac{3\sqrt{3}}{2}\ell(\Sigma_g\phi_g - \sum_{g'=1}^{G} W_{gg'}\phi_{g'}) = \sum_{i=1}^{6} I_g^i \quad . \tag{4.4}$$

$W_{gg'}$, is defined by Eq.(4.2), ℓ is the node side length. The RHS of Eq.(4.4) is invariant under the symmetries of the node, only the I_g^i's are transformed among each other. The same is true of the first term of the LHS. Hence only the component invariant under each symmetry transformation contributes to the average flux. In the integral balance only this component is included. As it is shown in Appendix A, the range of integration in Eq.(4.3) can be narrowed to the foundamental region, i.e. to the interval $0 \leq \infty \equiv \arg\underline{\xi} < \pi/3$. Over this interval we can choose $\underline{t}_i(\underline{\xi})$ arbitrarily. Practice has proved [61], [85] that the choice

$$\underline{t}_i(\underline{\xi}) = \delta(\underline{\xi} - \underline{e}_1)\underline{t}_i \qquad |\underline{e}_1| = 1 \qquad \arg(\underline{e}_1) = \pi/3 \quad , \tag{4.5}$$

is advantegeous. With this choice the solution is decomposed into linear combinations of exponentials with the 6 vectors pointing to node-corners in the exponent; they satisfy the DE (4.1) at each point:

$$\underline{f}_{ik}(\underline{x}) = e^{\lambda_k \underline{e}_i \underline{x}}\underline{t}_i \qquad i = 1,\ldots,6 \;\; ; \;\; k = 1,\ldots,G \quad . \tag{4.6}$$

The irreducible representations (see Appendix A), or shortly irreps are projected out by Eq.(A8). Since the exponential functions with different λ_k transform the same way, we have [85]

$$\underline{\Psi}_{ik} = \bar{\omega}_i \bar{f}_k \underline{t}_k \qquad i = 1,\ldots,6 \;\; ; \;\; k = 1,\ldots,G \quad . \tag{4.7}$$

where

$$\begin{aligned}
\bar{\omega}_1 &= (1,\ 1,\ 1,\ 1,\ 1,\ 1)/\sqrt{6} \\
\bar{\omega}_2 &= (1,\ -1,\ 1,\ -1,\ 1,\ -1)/\sqrt{6} \\
\bar{\omega}_3 &= (2,\ -1,\ -1,\ 2,\ -1,\ -1)/\sqrt{12} \\
\bar{\omega}_4 &= (0,\ 1,\ -1,\ 0,\ 1,\ -1)/2 \\
\bar{\omega}_5 &= (2,\ 1,\ -1,\ -2,\ -1,\ 1)/\sqrt{12} \\
\bar{\omega}_6 &= (0,\ 1,\ 1,\ 0,\ -1,\ -1)/2
\end{aligned} \tag{4.8}$$

and

$$\bar{f}_k = (e^{\lambda_k \underline{e}_1 \underline{x}}, e^{\lambda_k \underline{e}_2 \underline{x}}, \ldots, e^{\lambda_k \underline{e}_6 \underline{x}}) \quad . \tag{4.9}$$

The flux $\underline{\Psi}$ is a linear combination of the irreps:

$$\underline{\Psi}(\underline{x}) = \sum_{i=1}^{6} \sum_{j=1}^{G} b_{ij} \underline{\Psi}_{ij}(\underline{x}) \quad . \tag{4.10}$$

The 6G coefficients b_{ij} are to be determined from the irreps of the incoming currents:

$$\underline{m}_k = \sum_{i=1}^{6} \omega_{ki} \underline{I}_i \quad . \tag{4.11}$$

From Eq.(4.10) we have

$$\underline{m}_k = A_k \underline{b}_k \quad , \qquad k = 1,\ldots,6 \quad ; \tag{4.12}$$

where $\underline{b}_k = (b_{k1}, b_{k2},\ldots,b_{kG})$ and the matrices A_k are obtained by applying the definitions (3.7) (Ψ_g is substituted by $\underline{\Psi}_{ik}$) employing Eq.(4.7):

$$(A_1)_{k\ell} = \tfrac{1}{2}[2(\frac{1}{\lambda_\ell} + \gamma_{k\ell})\mathrm{sh}\lambda_\ell + (1 + \frac{2\gamma_{k\ell}}{\lambda_\ell})\mathrm{ch}\lambda_\ell - \frac{2\gamma_{k\ell}}{\lambda_\ell}]t_{k\ell} \quad , \tag{4.13}$$

$$(A_2)_{k\ell} = \tfrac{1}{2}[(1 - \frac{2\gamma_{k\ell}}{\lambda_\ell})\mathrm{sh}\lambda_\ell - (\frac{2}{\lambda_\ell} - 2\gamma_{k\ell})\mathrm{ch}\lambda_\ell + \frac{2}{\lambda_\ell}]t_{k\ell} \quad . \tag{4.14}$$

$$(A_3)_{k\ell} = \tfrac{1}{2}[(2\gamma_{k\ell} - \frac{1}{\lambda_\ell})\mathrm{sh}\lambda_\ell + (1 - \frac{\gamma_{k\ell}}{\lambda_\ell})\mathrm{ch}\lambda_\ell + \frac{\gamma_{k\ell}}{\lambda_\ell}]t_{k\ell} \quad , \tag{4.15}$$

$$(A_5)_{k\ell} = \tfrac{1}{2}[(1 + \frac{\gamma_{k\ell}}{\lambda_\ell})\mathrm{sh}\lambda_\ell + (\frac{1}{\lambda_\ell} + 2\gamma_{k\ell})\mathrm{ch}\lambda_\ell - \frac{1}{\lambda_\ell}]t_{k\ell} \quad , \tag{4.16}$$

where $\gamma_{k\ell} = 2D_k\lambda_\ell/(\sqrt{3}\cdot h)$. The missing matrices are

$$A_4 = A_3 \quad , \tag{4.17}$$

$$A_6 = A_5 \quad . \tag{4.18}$$

It is easy to check that only $\underline{\Psi}_{1k}$ contributes to the average flux, thus

$$\underline{\phi} = \tilde{W}\cdot\underline{b}_1 \tag{4.19}$$

and the matrix $\tilde{W}$ is given by

$$\tilde{W}_{k\ell} = \frac{4}{\sqrt{6}} \frac{1}{\lambda_\ell}(\mathrm{sh}\lambda_\ell + \frac{\mathrm{ch}\lambda_\ell - 1}{\lambda_\ell})t_{k\ell} \quad . \tag{4.20}$$

Let $\underline{n}_k$ denote the k-th irrep of the outgoing currents. Comparing Eq.(3.6) to Eq.(3.7) we get:

$$\underline{n}_k = A_k^* \underline{b}_k \tag{4.21}$$

and the matrix A_k^* is obtained from A_k by substituting $\gamma_{k\ell} \to -\gamma_{k\ell}$. Since the $\tilde{\omega}_i$ vectors form an orthonormal vector set, the outgoing currents at node face

k are formed from the irreps as

$$\underline{J}_k = \sum_{i=1}^{6} \omega_{ik} \underline{n}_k \quad , \qquad k = 1,\ldots,6 \quad . \tag{4.22}$$

Thus both the average fluxes and the outgoing currents can be expressed in terms of incoming currents:

$$\underline{\Phi} = \tilde{W} \cdot (A_1)^{-1} \underline{m}_1 \quad , \tag{4.23}$$

confer Eqs (3.3), (4.12) and (4.19), moreover

$$\underline{n}_k = R_k \underline{m}_k \equiv A_k^* A_k^{-1} \underline{m}_k \quad . \tag{4.24}$$

Finally, the outlined method can be summarized as follows: we start from the DE (4.1) whose analytic solution is Eq.(4.3). Alike most nodal methods, our method uses face-averaged partial currents as boundary condition. In Appendix A it is shown that the solution of the DE with fixed incoming currents at node-faces can be set up, solving the DE with symmetric boundary condition problems. Decomposing the exponentials in Eq.(4.3) into irreps, leads us to the required analytic solutions. The solutions in question involve an arbitrary weight function ($\underline{t}_1(\underline{r})$) which we chose as given in Eq.(4.5) in order to shorten the calculations. Only the unit representations (i.e. the irrep of highest symmetry) contributes to the average fluxes, see Eq.(4.23), and the irreps of the outgoing currents are given with the help of a diagonal response matrix, see Eq.(4.24), i.e. the different irreps do not mix together.

5. THE HEXAN PROGRAM

HEXAN is based on the principles given in the previous section. As to programing, HEXAN is a typical response matrix algorithm, the response matrices being determined by an analytic diffusion theory solution.

The basic quantity in the iterational process is the outgoind current. The initial guess is $\phi = 1$ and $J_i = 0.25$ (i=1,...,6) in each group. The iteration sweeps through the nodes, determining the new outcurrents from the last known incurrents. The number of sweeps is determined by the input. At the end of the last sweep the k_{eff} is evaluated from the balance. Since the response matrix elements are determined throughout k_{eff}, they are recalculated several times during the iterations. The last sweep ends an outer iteration step, the above procedure is repeated until convergence has been reached.

In each outer iteration the calculation begins by solving the eigenvalue problem (4.2). The subroutine EIGRF [83] is used here, on CDC machines the EISPACK program package is being used with success [84]. The response matrices R_k (see Eq.(4.24)), and the matrix W are determined for each material. The response matrix elements are stored on a disk unit, in a direct access file.

During the iteration all the fluxes and outgoing currents are kept in the central memory. The calculations in a given node begin by collecting the incoming currents. From the incoming currents the average fluxes and outgoing currents in each energy group are determined according to Eqs (4.23), (4.24) and (4.22).

The program employs only two accelerating methods:

a/ restrained overrelaxation [86]

The partial currents and average fluxes of a given node are determined from the freshly determined value (ϕ_n^*) as

$$\phi_n = \phi_n^* + Y \quad , \tag{5.1}$$

where

$$\begin{aligned} Z &= (\beta-1)(\phi_n^*-\phi_{n-1}) \\ X &= \min[\tfrac{1}{2}|\phi_n^*|, \phi_{n-1}] \\ Y &= \begin{cases} X & \text{if } Z > X \\ -X & \text{if } Z < -X \\ Z & \text{otherwise} \end{cases} \end{aligned} \tag{5.2}$$

and ϕ_{n-1} is the value from the previous iteration. The β parameter is chosen experimentally. It is known that β depends on the convergence radius. Among the test results we give examples, how this dependence appears.

b/ asymptotic extrapolation with restraint [86]

The asymptotic extrapolation was developed in relation to the GAUGE [87] program. When determining the eigenvalue problem

$$T\Psi = \lambda\Psi \tag{5.3}$$

we may use the following recursive method:

$$T\Psi^{(n)} = \lambda_n \Psi^{(n+1)} \tag{5.4}$$

with the initial guess $\lambda_o = 1$, $\Psi^{(o)} = 1$, and let us express $\Psi^{(o)}$ by means of the eigenvectors of operator T as

$$\Psi^{(o)} = \sum_{i=0}^{\infty} c_i \varphi_i \tag{5.5}$$

$T\varphi_i = \lambda_i \varphi_i$, $\max_i \lambda_i = \lambda$ and the corresponding φ_i is denoted by Ψ.
The n-th iteration gives:

$$\Psi^{(n)} = \Psi + \sum_{i=1}^{\infty} c_i \left(\frac{\lambda_i}{\lambda}\right)^n \varphi_i \quad . \tag{5.6}$$

If $\lambda_1/\lambda << 1$ and $n > 1$ we may resort to the approximation

$$\Psi^{(n)} = \Psi + c_1\left(\frac{\lambda_1}{\lambda}\right)^n \varphi_1 \quad . \tag{5.7}$$

The function $c_1\varphi_1$ is not known, but may be determined by applying the operator T to Eq.(5.7)

$$\begin{aligned} \Psi^{(n)} &= \Psi + R\sigma^n \quad , \\ \Psi^{(n+1)} &= \Psi + R\sigma^{n+1} \quad , \end{aligned} \tag{5.8}$$

where $R = c_1\varphi_1$ and $\sigma = \lambda_1/\lambda$. Thus we have

$$R = (\Psi^{(n+1)} - \Psi^{(n)})/(\sigma^{n+1} - \sigma^n) \quad , \tag{5.9}$$

$$\Psi = \Psi^{(n+1)} + \frac{\sigma}{1-\sigma}(\Psi^{(n+1)} - \Psi^{(n)}) \quad . \tag{5.10}$$

The restraint confines Ψ to positive values. The most advantageous values of the upper limit of $\sigma/(1-\sigma)$ and the parameter β in Eq.(5.2) should be determined experimentally.

The structure of HEXAN program is given in *Fig. 5.1*. The tasks solved by the named blocks of the flow-chart are listed below. Each block represents a subroutine.

MANAGER (1) Determines the addresses of the arrays in the data pool and reads the first card package of the input. The first package consists of five input groups, each given in name-list format (see input description). This program calls five subroutines (RASTER, XSECT, ALBEDO, SOLVE, EDITOR).

RASTER (2A) Performs the node-numbering, and calls three further subroutines (CHART, MULTIN, MATCH).

CHART (2A1) Prints data in map form (e.g. node-numbers, flux and power maps).

MULTIN (2A2) Reads in an integer array, consisting of pairs, as given in the input description.

MATCH (2A3) Fills out an array called IDEN. This array identifies the neighbours of the given node, e.g. IDEN (1,6) = the node-number of that node which is adjacent to 6-th face of node 1. For rotational symmetry it determines the corresponding neighbours of nodes situated at core edge: MATE1 enlists the neighbours of nodes with boundary condition 16, MATE2 of nodes with

boundary condition 17. The boundary condition types are given in page 37.
In the case of reflectional symmetry MATE1 and MATE2 specify the albedo indices necessary to form incurrents in corner nodes.

XSECT (2B) Reads in the cross-sections and fills the XTAB cross-section table.

ALBEDO (2C) Reads the extrapolation distances and converts them into albedos.

SOLVE (2D) Comprises the setting up of the initial guess (ϕ = 1.0 and J = 0.25 in each node in each group) as well as the outer iteration. The iteration begins with the determination of the X-section matrix elements (in subroutine MATRIX), see Eq.(4.2) the eigenvalue problem (4.2) is solved by EIGRF. The response coefficients, see Eq.(4.24), are determined in the COEFF subroutine, according to Section 4. The inversion of the matrices A_i (cf. Eqs (4.13)-(4.16)) is performed by subroutine MI. In MATMAT the matrix product $A_k^* A_k^{-1}$ is determined (see Eq.(4.24)). In the case of complex eigenvalues the real and imaginary part of the response matrices are composed in subroutine CMPLIX. The response matrix elements are kept in a direct access file. After sweeping through all the nodes NIT times, the eigenvalue k_{eff} is determined, from the reaction rates given by EXTRAP, and here ends an outer iteration step.

SCAN (3D) Takes each node, in each node each group, in turn. First the actual response matrix elements are retrieved from the DA (= direct access) file, then the incoming currents of the actual node are collected. The irreps of the incoming currents are determined by VMULT according to Eq.(4.11). The irreps of the outgoing currents determined in MATVEC, see Eq.(4.21). The outcurrents are reconstructed in VMULT, see Eq.(4.22). At the determination of the new outcurrents and average fluxes an overrelaxation is used with restraint in subroutine RESTRT. The formulas are given in Section 5.

EXTRAP (3E) Determines the leakage rate, the absorption and fission rates to allow the determination of k_{eff} from the balance. The asymptotic extrapolation is carried out here. The extrapolation parameters are determined from outer iterations. The last known flux and partial currents are written into the DA file mentioned before.

EDITOR (2E) Prints the results, determines the balance in each node.

The HEXAN program was written in FORTRAN-IV extended language. The following libraries are needed:

a/ SOFT.CERN.LOADLIB
b/ SYS1.FORTLIB
c/ SYS2.FORTLIB
d/ SOFT.IMSL.LOADLIB

HEXAN needs 175k central memory, approximately 30-cylinder work area on a disk unit. The program resides on a MT of serial number 000117, its parameters are LABEL=(18,SL),DCB=(FB,80,800).

6. INPUT AND OUTPUT DESCRIPTION

All input information comes from cards. No other input, e.g. x-section library, is allowed. The reactor to be calculated by HEXAN has a given structure fixed in a so-called map that specifies the relative positions of the nodes, see *Fig. 6.1*. The map consists of columns and rows; nodes with a given vertical (horizontal) coordinate form a row (column). The nodes are numbered either columnwise or spirally. IN THE CASE OF ROTATIONAL SYMMETRY SPIRAL ORDERING IS PROHIBITED.

The node-faces are numbered in a fixed way, shown in *Fig. 6.2*. Node--faces not adjacent to other node are called free node-faces. On free node--faces some boundary condition must be given allowing one to generate incurrents from outcurrents. The accepted boundary condition types are enlisted in Table 6.1. The identification of matching node-faces goes sequentially in the case of rotational symmetry, thus MATE1 (i) gives the node number matching to the i-th boundary with boundary condition 16.

Every node is filled with a material identified by material number. A material number means a set of cross-sections collected in the x-section table, having RSYST format [88].

The process of the calculation is divided into outer and inner iterations. Since all energy groups are considered simultaneously, the inner iteration in HEXAN means a sweep through the nodes without determining new k_{eff}. Calculations between two determinations of k_{eff} form an outer iteration step. The response matrix elements depend on k_{eff} but a parameter (NCOEFF) determines the frequency of their redetermination, NCOEFF=1 means to determine new response matrix elements in each outer iteration. Convergence has been reached when $|\Delta k_{eff}| <$ EPS1 and the error in fission sources (S) is smaller than EPS1, and $|\Delta\phi| <$ EPS2. If convergence has been reached MAXI is doubled and 3 further outer iteration step is performed.

The input often contains numbers repeated several times. In such cases there is a possibility of shortening the input by using the format (NREPI,ITEMI), which means ITEMI is repeated NREPI times (ITEMI may be either real or integer).

The input consists of 3 packages.

1. PACKAGE: Task identification string and namelist cards

CARD NO.	NAMELIST	VARIABLE	MEANING
1	-----	ID	identification string
2	MAP1	LMAX	number of nodes
		NCOL	number of columns in node map
		NFREE	number of free node surfaces where IDEN (1,i) < 0
		TEMP	>0 flat-to-flat node size in cm <0 node side length, in cm
3	MAT2	NMAT	number of materials
		IGM	number of energy groups (<7)
4	XTAB3	IHT	position of total x-section in x-section table
		IHS	position of self-scattering x-section
		IHM	length of x-section table
		NUS	upscattering range
5	ITER4	MAXI	number of sweeps per outer iteration
		MAXO	max. number of outer iteration
		NCOEFF	frequency of coefficient recalculation
		IPRIN	printing option: 0---basic print (see output) $\geq$2--node balance table is printed
		INIT	sweep number where overrelaxation is switched on
		WEIGHT	weight for overrelaxation
6	KONV5	EPS1	error limit for k_{eff} and source
		EPS2	error limit for flux

2. PACKAGE: Map specifications

Nodes are numbered either columnwise or spirally. In the case of columnwise numbering the positions of the lowest and uppermost nodes in the column determine the mode of numbering. When spiral numbering is used, on the 2nd--5th boundaries of the central node a boundary condition of type 10 should be prescribed, see Table 6.1.

WARNING: SPIRAL ORDERING IS PROHIBITED WHEN ROTATIONAL BOUNDARY CONDITION IS USED. In this case the use of upward numbering is strongly advised.

CARD NO.	VARIABLE	MEANING
1	(II(I),JJ(I), I=1,NCOL+1)	Position of uppermost and lowest nodes in column I.
The node numbering is determined as follows: a/ II(NCOL+1)=0 when II(I)<JJ(I) the I-th column is numbered from top to bottom, when II(I)>JJ(I) the I-th column is numbered from bottom to top. b/ II(NCOL+1)≠0. spiral ordering is used, the centre of the spiral is (II(NCOL+1),JJ(NCOL+1)) and II must always be smaller than JJ.		
2	(MAT(K),K=1,LMAX)	Material map. Each node is filled with a given material. The LMAX material numbers are given according to increasing node numbers. The format (NRI,ITI) may be used if ITI is repeated NRI times.
3	(IBOUND(K),K=1, K=1,NFREE)	Boundary condition type. The format is (NRI,ITI), when the I-th item is repeated NRI times.
Boundary condition types are given in Table 6.1.		

3. PACKAGE: Cross-sections

CARD NO.	VARIABLE	COMMENT
1	N	material number
2	(SIG(n,IG,I), ,IG=1,IGM,I=1,IHM)	cross-section table in RSYST [88] format: 1. fission 2. any entry ⋮ IHT-3 transport x-section IHT-2 absorption IHT-1 multiplication IHT total x-section IHT+1 upscattering ⋮ IHS-2 IHS-1 IHS self scattering IHS+1 downscattering IHS+2 ⋮ IHM
3	(CHI(n,IG),IG=1,IGM)	fission spectrum
Cards 1-3 are repeated NMAT times.		
4	(ALB(K,IG),K=1,IALB, IG=1,IGM)))	Albedos for the boundaries where IBOUND=3 was specified the albedos follow according to increasing node number, within a node according to increasing face number.

The face numbering in a node is shown in *Fig. 6.2*. The parameters NDS and IALB are determined by the program from other input data.

The output consists of the basic print:

a/ heading, it is the identification string ID, see input
b/ the content of the namelist cards
c/ map of numbered nodes
d/ boundary condition table
e/ material map
f/ cross-section table
g/ central memory statistics
h/ iteration monitor
i/ group neutron balance for the whole system
j/ total neutron balance for the whole system

k/ unnormalized nodal fluxes in each group
l/ normalized power distribution
m/ normalized nodal fluxes in each group
n/ normalized power distribution map
o/ total CP time and a termination message
additional output, when IPRIN≥2, (see input)
p/ nodewise balance for every group

7. TEST RESULTS

a/ MARAKAZOV'S BENCHMARK [25]

This benchmark problem is a two-group WWER-440 model problem, for which solutions of several programs are available. Specification of the problem is given in Ref. [25]. The core is made up of hexagons with 8.4868 cm node side length, the material in the nodes is one of the 3 fissionable mixtures corresponding to different enrichments. Along two sides of the core reflective boundary condition is prescribed, along the third side a reflector is taken into account by extrapolation distances.

HEXAN probably overestimates the k_{eff} by 4×10^{-4}. The power distribution shows a larger than 1 % difference along the boundary where albedo boundary condition is used. As reference, the finite element KRESOMISL code, using 48 point/node, may be taken for this benchmark. Comparison with other results is given in Table 7.1.

b/ WWER-1000 BENCHMARK

The zone consists of 38 nodes, filled with 4 materials: 3 differently enriched fuel and a reflector. The node side length is 8.086425 cm. This benchmark is a challange owing to spectral effects in nodes close to reflector as well as owing to the large node size compared to the termal cross-sections. The benchmark problem is specified in Table 7.2.

HEXAN solved the problem in 128.6 sec (EC-1040 computer), completing 26 outer iterations and the eigenvalue obtained is $k_{eff} = 1.11209$ with $\Delta k_{eff} = 3\times10^{-6}$ and $\Delta\phi = 8\times10^{-5}$. Table 7.3 illustrates the impact of the overrelaxation weight on the convergence. $\Delta\phi$ means the flux error in the last iteration. The convergence limit was 10-3 but the program having reached this limit performs three further iterations with doubled ITI value (see input).

c/ GENERAL ATOMICS BENCHMARK [89]

Hexagonal geometry is used in high temperature gas cooled reactors (HTGR) as well. This benchmark models a HTGR. The core contains 7 materials:

a/ controlled core
b/ uncontrolled core
c/ regular core

d/ buffer core, one side on core reflector boundary
e/ buffer core, two sides on core reflector boundary
f/ buffer core, three sides on core reflector boundary.

Each material is described in four energy groups with down-scattering only. The core has a 60 degree rotational symmetry. The node side length is 20.90 cm. Detailed specification of this problem can be found in Ref. [89]. Results are shown in Table 7.4. The reference eigenvalue is $k_{eff} = 1.1183$, obtained by extrapolation to zero mesh-size [90]. The effect of the overrelaxation weight on convergence is shown in Table 7.5. An approximate comparison of different computers is

1 sec IBM 360/195 = 2 sec IBM 360/91 = 4 sec CYBER 174 ≙ (11 sec UNIVAC 1108) = 30 sec EC-1040.

8. CONCLUSIONS

We have presented a new nodal method. In Section 4 it has been shown that an analytic solution is available in a homogeneous node. We were able to derive such a form of this solution which is applicable to any geometry. We were able to construct the solution of the DE by considering solely symmetrized problems, moreover these symmetrized problems have an analytic solution, see Eq.(A21). In the analytic solution a weight function appears, that was chosen in accordance with the use of face-averaged partial currents, see Eq. (4.5). By means of these analytic solutions to the symmetric problems, the response matrix elements are determined as given by Eqs (4.13)-(4.18) and (4.24). Since the above solutions are eigenfunctions of every symmetry of the hexagon (or in mathematicians' terminology they are irreducible with respect to the symmetry group C_{6v}), the response matrix will be diagonal.

Merit of the above idea has been shown in Section 7, by the test results of the HEXAN program. The few accelerating gadgets built into HEXAN are described in Section 6. It is clear from the presented theory, that HEXAN is limited by the use of face-averaged partial currents alone. The test results show that further accelerating methods are needed and the role of the weight factor in the overrelaxation should be clarified.

APPENDIX A: SYMMETRIES APPLIED TO BOUNDARY-VALUE PROBLEMS

The invariance of the differential equations of physics under some group of transformations is one of the most important properties of these equations. The benefit of the symmetry properties lies, among others, in finding a suitable set of independent variables for the equation considered or in establishing conservation relations. Lie proposed a systematic method [92] for searching for the groups of symmetry of differential equations. The main

achievements of this field are summarized in an excellent book by Ovsjannikov [93]. A salient result is the Noether theorem, which determines the conservation law from infinitesimal transformations. Recently the inclusion of non-local symmetries [94], [95], the extension to integro-differential equations [96] and the corresponding generalizations of the Noether theorem are in the focus of interest. In boundary-value problems, however, it is not the conservation law but the method for finding the irreducible representations what is required, since an important physical meaning can be rendered to the irreducible representations (irreps).

It will be shown that boundary-value problems of a linear operator involving derivation can be solved by finding the solutions of symmetrized boundary condition problems, and the solution is an irreducible representation. It is shown that any boundary condition problem can be expressed as a sum, in which each term is such that the corresponding boundary condition is multiplied with the corresponding irrep. Since symmetry considerations are scarcely ever used in reactor physics we begin with the symmetries [97], [98].

Assume that we are given an equation

$$\hat{O}f(\underline{x}) = 0 \quad , \tag{A1}$$

$\underline{x}$ being the independent variable, $\hat{O}$ a linear operator. We shall call symmetry of $\hat{O}$ any prescription $\hat{P}$ permitting us to transform any solution $f(\underline{x})$ into another solution $\hat{P}f(\underline{x})$. Before proceeding we give examples:

$$\text{a/} \quad \hat{O} = (\underline{\nabla} + \Sigma) \quad .$$

In this case symmetry is any orthogonal coordinate transformation and any translation.

$$\text{b/} \quad \hat{O} = (-D\underline{\nabla}^2 + \Sigma) \quad .$$

The symmetries are the same as above. The considered symmetries attach to coordinate transformations. The transformation operator $\hat{P}_R$ associated with the coordinate transformation R is defined by the following operator equation that must be an identity in $\underline{x}$:

$$\hat{P}_R f(\underline{x}) \equiv f(R^{-1}\underline{x}) \quad . \tag{A2}$$

It must be emphasized that the operator acts upon the coordinate x and not upon the argument of f.

If $\hat{P}_R\hat{P}_S$ is defined to mean "P_S operates first and then $\hat{P}_R$ operates", then the set of symmetries $\{\hat{P}_R\}$ is isomorphic with the set of coordinate transformations {R}. If {R} is the set of all symmetry transformations of the operator $\hat{O}$, then P_R commutes with $\hat{O}$

$$\hat{P}_R\hat{O} = \hat{O}\hat{P}_R \qquad (A3)$$

for all R and the set $\{\hat{P}_R\}$ is a group, denoted by G. To find relationship between $f(\underline{x})$ and $f(R^{-1}\underline{x})$ first a suitable basis is chosen. The formal solutions of Eq.(A1) span a function space. In this space a sub-space V_s is called invariant sub-space if we can find a matrix $\Gamma(R)$ for every $\hat{P}_R$ in G, of scalar coefficients such that

$$\hat{P}_R\underline{\varphi}_i = \Gamma^{(i)}(R)\underline{\varphi}_i \quad , \quad \underline{\varphi}_i \in V_s \quad . \qquad (A4)$$

A change of the basis vectors $\underline{\varphi}_i$ amounts to nothing more than an equivalence transformation on $\Gamma^{(i)}$. The set of matrices $\{\Gamma^{(i)}(R)\}$ is isomorphic with the group G. To distinguish inequivalent representations we introduce the character: the characters of a representation i are the traces of the matrices of the representation:

$$\chi^{(i)}(R) = \sum_k \Gamma^{(i)}(R)_{kk} \quad , \qquad (A5)$$

where the representations are labelled by superscript i. The dimension of the matrices $\Gamma^{(i)}(R)$ depend on the dimension of the basis vector $\underline{\varphi}_i$ in Eq (A4). If its dimension equals the number of elements in group G, the representation is called regular. There is a specific relationship between the matrices $\Gamma^{(i)}(R)$ and the basis vector $\underline{\varphi}_i$: if there exists a similarity transformation bringing every $\Gamma^{(i)}(R)$ into block diagonal from simultaneously, then there exist sub-space in V_s, each of which is transformed into itself by the group G. In this case the sub-space spanned by $\underline{\varphi}_i$, as well as the corresponding representation $\{\Gamma^{(i)}(R)\}$ are called reducible, otherwise irreducible. It has been shown [97], [98] that any function can be decomposed into components transforming according to irreps:

$$\underline{\Psi}(\underline{x}) = \sum_i c_i \Psi_i(\underline{x}) \qquad (A6)$$

and $\Psi_i(\underline{x})$ is irreducible, moreover the different irreps are orthogonal:

$$(\Psi_i, \Psi_j) = 0 \qquad \text{if} \quad i \neq j \quad . \qquad (A7)$$

Hence finding block diagonal metrices $\Gamma^{(i)}(R)$ and finding an invariant sub-space in V_s are equivalent problems. The irreps have exhaustively been studied and their properties are summarized in a so-called character table, which is a square table, useful in finding the irreps of a given group according to the following recipe:

$$\hat{P}^{(i)}\Psi = \frac{\ell_i}{h}\sum_R \chi^{(i)}(R)^* \hat{P}_R(\Psi) \quad , \qquad (A8)$$

where

ℓ_i - dimension of the i-th irrep

$\chi(R)^*$ - is the adjoint to the matrix formed from the character table

h - number of elements in (the order of) group G.

Character tables of different groups are available in textbooks [98].

Let us consider the boundary-value problem

$$\hat{O}f(\underline{x}) = 0 \qquad \underline{x} \in V \tag{A9a}$$

$$\hat{B}f(\underline{x}) = g(\underline{x}) \qquad \underline{x} \in \partial V \tag{A9a}$$

where $\hat{B}$ is a linear operator such that if $\hat{O}\hat{P}_R = \hat{P}_R\hat{O}$ then $\hat{B}\hat{P}_R = \hat{P}_R\hat{B}$. The irreps of function $g(\underline{x})$ can be determined as

$$g_i(\underline{x}) = \frac{\ell_i}{h}\sum_{R\in G}\chi^{(i)}(R)^* g(R^{-1}\underline{x}) \quad . \tag{A10}$$

Since $g_i(\underline{x})$ is an irreducible representation,

$$\hat{P}_R g_i(\underline{x}) = \lambda_R^{(i)} g_i(\underline{x}) \quad , \tag{A11}$$

where $\lambda_R^{(i)}$ is the element $\chi^{(i)}(R)$ of the character table. The boundary-value problem

$$\hat{O}f_i(\underline{x}) = 0 \qquad \underline{x} \in V \tag{A12a}$$

$$\hat{B}f_i(\underline{x}) = g_i(\underline{x}) \qquad \underline{x} \in \partial V \tag{A12b}$$

is easier to solve, owing to the symmetric boundary condition, than the original problem (A9). By means of the linearity of operators $\hat{O}$ and $\hat{B}$,

$$f(\underline{x}) = \sum_i c_i f_i(\underline{x}) \quad , \tag{A13}$$

thus we were able to express the solution to Eq.(A9) in terms of solutions to Eqs (A12). The function $f_i(\underline{x})$ is an irrep of f as it will be shown below. It comes from Eqs (A10) and (A12) that on the boundary $f_i(\underline{x})$ transforms as $g_i(x)$:

$$\hat{B}\hat{P}_R f_i(\underline{x}) = \hat{P}_R\hat{B}f_i(\underline{x}) = \hat{P}_R g_i(\underline{x}) = \lambda_R^{(i)} g_i(\underline{x}) = \hat{B}(\lambda_R^{(i)} f_i(\underline{x})) \qquad \underline{x} \in \partial V \quad .$$

Assuming that any solution of Eq.(A1) must be continuous inside the region V, let us consider a point x lying close to the boundary and write

$$f_i(\underline{x}) = f_i(\underline{x}_b) + h_i(\underline{x},\underline{x}_b) \quad , \tag{A14}$$

where $\lim_{\underline{x}\to\underline{x}_o} h(\underline{x},\underline{x}_b) = 0$, and $\underline{x}_b \in \partial V$. Let the new coordinate after the transformation R be

$$\underline{x}' = R\underline{x} \qquad\qquad \underline{x}_b' = R\underline{x}_b \quad .$$

Applying $\hat{P}_R$ to Eq.(A14) we have

$$f_i(\underline{x}') = f_i(\underline{x}_b') + h_i(\underline{x}';\underline{x}_b') \tag{A15}$$

and assuming that our statement is wrong there exists a transformation such that

$$\hat{P}_R f_i(\underline{x}) \neq \lambda_R^{(i)} f_i(\underline{x}) \quad .$$

Substituting Eq.(A11) into Eq.(A15) we have

$$\lim_{\underline{x}' \to \underline{x}_b'} [f_i(\underline{x}') - f_i(\underline{x}_b')] \neq 0 \quad .$$

But on the other hand:

$$\lim_{\underline{x}' \to \underline{x}_b'} h(\underline{x}';\underline{x}_b') = 0 \quad ,$$

what is a contradiction, thus it has been shown that the irreps of the problem (A9) can be obtained by solving the "symmetrized" problems that are formed by substituting the boundary conditions with its irreps in turn. In reactor physics a widely used boundary condition is the incoming current given along the boundary. For simplicity's sake we assume that the considered node is adequately described by face-averaged partial currents. To find the physical meaning of the irreps, the incoming current vector of a square node is decomposed according to Eq.(A8):

$$\begin{bmatrix} I_1 \\ I_2 \\ I_3 \\ I_4 \end{bmatrix} = \frac{I_1+I_2+I_3+I_4}{4}\begin{bmatrix} 1 \\ 1 \\ 1 \\ 1 \end{bmatrix} + \frac{I_1-I_2}{2}\begin{bmatrix} 1 \\ -1 \\ 0 \\ 0 \end{bmatrix} + \frac{I_3-I_4}{2}\begin{bmatrix} 0 \\ 0 \\ 1 \\ -1 \end{bmatrix} + \frac{I_1+I_2+I_3+I_4}{4}\begin{bmatrix} 1 \\ 1 \\ -1 \\ -1 \end{bmatrix} \tag{A16}$$

thus the solution of the four symmetrized problems means

a/ Finding the neutron distribution in a cell lying in a homogeneous surrounding. This solution corresponds to the unit representation that is invariant under every symmetry transformation. Only this solution contributes to the average flux.

b/ Finding the neutron distribution in a cell imbedded into a constant stream along the x direction.

c/ Finding the neutron distribution in a cell imbedded into a constant stream along the y direction. If the cell is symmetric, this solution is same as item b/. Solutions of items b/ and c/ form the components of the so-called dipole type cell function.

d/ Finding the neutron distribution in a cell imbedded into a cross-flow: in-stream from x direction and out-stream to y direction. This solution is called quadrupole type cell function.

As to the magnitude of the above solutions, numerical evidence attests to component a/ being dominant; component b/ or c/ may have some importance in nodes by the reflector-core boundary. It is worth noting that the above obtained decomposition gives the rigorous foundation for several homogenization schemes.

As it has been shown in Section 4, the solution of Eq.(4.1) is

$$\underline{\Psi}(\underline{x}) = \sum_{i=1}^{G} \int_{|\underline{\xi}|=1} \underline{t}_i(\underline{\xi}) e^{\lambda_i \underline{\xi}\underline{x}} d\underline{\xi} \quad ,$$

here this function will be decomposed into irreps. The symmetries of the hexagon form the group C_{6v}, they are enrolled in Table A.1. To find the irreps we have to find the transforms of $e^{\lambda_i \underline{\xi}\underline{x}}$. Using Eq.(A2), and remembering that the symmetry transformations are orthogonal transformations we have

$$\hat{P}_R(e^{\lambda_i \underline{\xi}\underline{x}}) = e^{\lambda_i (R^{-1}\underline{\xi})\underline{x}} \quad , \tag{A17}$$

and since $\{R^{-1}\underline{\xi}\}$ covers the interval $|\underline{\xi}| = 1$ when $0 \leq \arg(\underline{\xi}) < \pi/6$ the integration can be narrowed to the interval called foundamental region [99]

$$\underline{\Psi}(\underline{x}) = \sum_{i=1}^{6} \int_{0}^{\pi/6} \underline{t}_i(\alpha) e^{\lambda_i \underline{\xi}(\alpha)\underline{x}} d\alpha \quad . \tag{A18}$$

The irreps of the function $e^{\lambda_i \underline{\xi}(\alpha)\underline{x}}$ are obtained with the help of the projector (A8). Every irrep will be a linear combination of exponential functions, as given by Eq.(A17). Let us choose a vector in the foundamental region. Its position is denoted by E in Table A.1. Carrying out the projection we obtain

$$S_i^{(k)}(\underline{x},\alpha) = \sum_{j=1}^{12} \omega_{kj} e^{\lambda_i \underline{\xi}_j \underline{x}} \quad , \tag{A19}$$

and the ω_{kj} matrix is orthogonal: its rows are orthogonal vectors. Its row vectors

$$\bar{\omega}_k = (\omega_{k1}, \omega_{k2}, \ldots, \omega_{k12})$$

are

$$\bar{\omega}_1 = \frac{1}{\sqrt{12}}(1,1,1,1,1,1,1,1,1,1,1,1)$$

$$\bar{\omega}_2 = \frac{1}{\sqrt{12}}(1,-1,1,-1,1,-1,1,-1,1,-1,1,-1)$$

$$\bar{\omega}_3 = \frac{1}{\sqrt{12}}(1,1,-1,-1,1,1,-1,-1,1,1,-1,-1)$$

$$\bar{\omega}_4 = \frac{1}{\sqrt{12}}(1,-1,-1,1,1,-1,-1,1,1,-1,-1,1)$$

$$\bar{\omega}_5 = \frac{1}{\sqrt{12}}(2,0,-1,0,-1,0,2,0,-1,0,-1,0)$$

$$\bar{\omega}_6 = \frac{1}{\sqrt{12}}(0,-1,0,-1,0,2,0,-1,0,-1,0,2)$$

$$\bar{\omega}_7 = \frac{1}{\sqrt{12}}(0,2,0,-1,0,-1,0,2,0,-1,0,-1) \qquad \text{(A20)}$$

$$\bar{\omega}_8 = \frac{1}{\sqrt{12}}(-1,0,2,0,-1,0,-1,0,2,0,-1,0)$$

$$\bar{\omega}_9 = \frac{1}{\sqrt{12}}(2,0,1,0,-1,0,-2,0,-1,0,1,0)$$

$$\bar{\omega}_{10} = \frac{1}{\sqrt{12}}(0,-1,0,1,0,2,0,1,0,-1,0,-2)$$

$$\bar{\omega}_{11} = \frac{1}{\sqrt{12}}(0,2,0,1,0,-1,0,-2,0,-1,0,1)$$

$$\bar{\omega}_{12} = \frac{1}{\sqrt{12}}(1,0,2,0,1,0,-1,0,-2,0,1,0)$$

This representation of the group C_{6v} is a regular one. There are four one-dimensional representations $(\bar{\omega}_1,\ldots,\bar{\omega}_4)$ and two two-dimensional ones. Since two-dimensional irreps occure twice in a regular representation, the four representations of the class Γ_5, i.e. $\bar{\omega}_5,\ldots,\bar{\omega}_8$ contain only two vector pairs which are equivalent for they are transformed into each other by similarity transformations. Equivalent representations have the same character determined by Eq.(A5). Hence the pair $\bar{\omega}_5,\bar{\omega}_6$ is equivalent to the $\bar{\omega}_7,\bar{\omega}_8$ pair. The flux is given by

$$\underline{\Psi}(\underline{x}) = \sum_{i=1}^{G} \int_0^{\pi/6} \underline{t}_i(\alpha) \sum_{k=1}^{12} c_k S_i^{(k)}(\underline{x},\alpha)\,d\alpha \quad , \qquad \text{(A21)}$$

and the twelve c_k as well as the $\underline{t}_i(\alpha)$ should be determined from the boundary condition: from the given incoming current at each point of the boundary. The use of face-averaged incoming currents not only considerably reduces the complexity of expression (A21), but it results in a satisfactory accuracy as well. There are several ways of reducing Eq.(A21). First of all the twelve classes are to be reduced to six as we have only six incoming currents. It can be done by choosing a special position for $\underline{\xi}_1$: when $\underline{\xi}_1$ is in the plane m_2' or in plane m_2, six of the vectors $\bar{\omega}$ turn to zero. The former choice has been found more advantageous. In this case the non-zero vectors $\bar{\omega}$ are given by Eq. (4.8).

APPENDIX B: RESPONSE MATRIX OF A SYMMETRIC NODE

Throughout all the preceding sections we dealt with the DE. In this section, however, the response matrix of a symmetric node is discussed and since the response matrix mathod is not necessarily confined to diffusion theory, the results will be valid for the TE (transport equation) as well [100]. This general character of the response matrix equations (RME) allows one to relate the RME with the nodal equations [67], [101] (cf. Eq.(3.14)). It will be shown that the irreps of the incoming currents in the node satisfy a nodal equation, similar to the FD equations. The coefficients in these nodal equations are derived from the response matrices of the node. In this section we use only one partial current per node-face that may cause some limitations. The inner structure of the node is assumed to be invariant under the symmetry transformations of the node. This assumption is frequently fulfilled though in large nodes for example the tilted burn-up effect is not in accordance with the above assumption.

In the previous section we have defined the irreps as such solution to the TE which are eigenfunctions of the symmetries of the node. The irreps have useful properties: they are orthogonal and form a complete set thus any function may be decomposed into irreps. Moreover, the irreps can be found by solving the TE with "symmetric" boundary conditions. Further important properties derive from the linearity of the projection (A8), and from the symmetric structure of the node. Several reaction rates are formed from the flux, such as

$$I_i = \frac{1}{F_i}\int_{F_i}\int_{\underline{\Omega}\underline{n}<0} -\underline{n}\underline{\Omega}\Psi(\underline{x},\underline{\Omega})\,d\underline{\Omega}\,dF_i \quad \text{- averaged incoming current} \tag{B1}$$

$$J_i = \frac{1}{F_i}\int_{F_i}\int_{\underline{\Omega}\underline{n}>0} \underline{\Omega}\underline{n}\Psi(\underline{x},\underline{\Omega})\,d\underline{\Omega}\,dF_i \quad \text{- averaged outcoming current} \tag{B2}$$

$$J_i^{net} = \frac{1}{F_i}\int_{F_i}\int_{4\pi} \underline{\Omega}\underline{n}\Psi(\underline{x},\underline{\Omega})\,d\underline{\Omega}\,dF_i \quad \text{- averaged net current} \tag{B3}$$

$$A_k(\underline{x}) = \int_{4\pi} d\underline{\Omega}\Sigma_k(\underline{x},\underline{\Omega})\Psi(\underline{x},\underline{\Omega})\,d\underline{\Omega} \quad \text{- reaction rate} \tag{B3}$$

and the above reaction rates belong to the same irrep as $\Psi(\underline{x},\underline{\Omega})$ does. Thus if the boundary condition fixes I = 1 at each face, the outgoing currents, the normal component of the net currents will be the same at/on the node faces, and the reaction rates will be invariant under every symmetry of the node.

The RME is written as

$$\bar{J} = R\bar{I} \quad , \tag{B5}$$

where the face-averaged incurrents, as well as outcurrents, have been contracted into a vector denoted by bar ($\bar{}$). The following trivial properties are immediate consequence of the properties of irreps:

a/ Let the irrep be determined as

$$\bar{i} = V\bar{I} \quad , \tag{B6}$$

$$\bar{j} = V\bar{J} \quad , \tag{B7}$$

then the response matrix Q defined by

$$\bar{j} = Q\bar{i} \tag{B8}$$

is diagonal.

b/ The R matrix has $m = (1 + ENT(\frac{n}{2}))$ independent elements, where n is the number of the node-faces. The independent elements are r-reflection, $\underline{t}_i$--transmission with i-face jumps, $i=1,\ldots,ENT(\frac{n}{2})$.

c/ The rows in matrix R are permutations of the above m elements.

d/ A symmetry transformation of the node may be equivalenced to a permutation of the node-faces. If P denotes this permutation matrix then

$$PR = RP \quad . \tag{B9}$$

e/ The matrices R and Q are related as

$$Q = VRV^{-1} \quad . \tag{B10}$$

f/ The matrix V, which brings the response matrix R into diagonal form is determined by the irreducible vectors $\bar{\omega}_i$. For hexagonal node a 12-element representation is given by Eq.(A20), a six-element representation by Eq.(4.8). It is remarkable that vectors show certain arbitrariness caused by the presence of 2-dimensional irreps. The matrix V formed from Eq.(4.8) is orthogonal, i.e.: $V^{+} = V^{-1}$.

g/ Only the unit representation gives non-vanishing contribution to the average flux (see Eq.(3.3)).

Acquainted with the above properties of a symmetric node's response matrix, we would pass on to relating RME and nodal equations. The attractive behaviour of the nodal equations [66] as well as the high accuracy and flexibility of the RME may motivate the search for a nodal equation with the RME's accuracy. First the notation should be changed in order to simplify the resulting expressions. To this end the following changes are made in the notation:

$\bar{i} \rightarrow \bar{X}^{(\ell)} = (X_1^{(\ell)}, X_2^{(\ell)}, \ldots)$ irreps of incoming current in the ℓ-th node

$\bar{j} \rightarrow \bar{Y}^{(\ell)} = (Y_1^{(\ell)}, Y_2^{(\ell)}, \ldots)$ irreps of the outgoing currents in the ℓ-th node.

Q is kept, its elements are determined by

$$Y_i^{(\ell)} = Q_i^{(\ell)} X_i^{(\ell)} \quad . \tag{B11}$$

To avoid the difficulties associated with the general analysis, a particular case will be followed. Let us consider a hexagonal node, the irreps being given by the vectors $\bar{\omega}_i$ in Eq.(4.8), and let us remember that now the V matrix, formed from the $\bar{\omega}_i$ vectors, is orthogonal [85]. The node numbering is given in *Fig. B.1*. The node sides are numbered in the same way in each node starting from the nord-east node-face, proceeding counterclockwise.

The ℓ-th irrep of the incoming current in the central node is

$$\bar{X}_\ell^{(o)} = \sum_{k=1}^{6} V_{k\ell} I_k^{(o)} \quad , \tag{B12}$$

and

$$I_\ell^{(o)} = J_{\ell'}^{(\ell)} \qquad \ell' = 1 + \mathrm{MOD}(\ell+2,6) \quad . \tag{B13}$$

The outcurrents are constructed from the irreps as

$$J_{\ell'}^{(\ell)} = \sum_{m=1}^{6} V_{\ell' m} Y_m^{(\ell)} \quad . \tag{B14}$$

We have from Eqs (B12) and (B14) by means of the RME

$$X_k^{(o)} = \sum_{\ell=1}^{6} V_{k\ell} \sum_{m=1}^{6} \omega_{\ell' m} Q_m^{(\ell)} X_m^{(\ell)} \qquad k=1,\ldots,6 \tag{B15}$$

Eq.(B15) is a linear expression of the central node's irreps (upper index o), and its six neighbours (upper index 1,...,6). We have 6 unknowns in each node (e.g. $X_\ell^{(o)}$, $\ell = 1,\ldots,6$). Let us introduce the notation

$$S_k^{(o)} = \sum_{\ell=1}^{6} \omega_{k\ell} \sum_{m \neq k} \omega_{\ell' m} Q_m^{(\ell)} X_m^{(\ell)} \quad , \tag{B16}$$

$$D_{k\ell} = \omega_{k\ell} \omega_{\ell' k} Q_k^{(\ell)} \quad , \tag{B17}$$

we have now

$$\sum_{\ell=1}^{6} [D_{k\ell} X_k^{(\ell)} - \tfrac{1}{6} X_k^{(o)}] = S_k^{(o)} \quad , \tag{B18}$$

what is a nodal equation indeed. The LHS is a linear expression of the k-th irrep of the central node and its neighbours, whereas the source is composed of other irreps. The set of equations (B18) cries for an iterative way of

solution. Let us start from the guess $X_k^{(\ell)} = \delta_{k1}$ for each ℓ. Sweeping throughout all the nodes, improves values of $X_1^{(\ell)}$, $\ell = 1,2,\ldots,N$ (= number of nodes in the problem) are determined. The sources occurring in the equation for $X_2^{(\ell)}$ are updated, and in the second sweep Eq.(B18) is solved for $k = 2$, $\ell = 1,\ldots,N$, and so forth. It is important that different irreps may considerably differ. The unit representation prevails almost everywhere as it can be seen that the difference of the partial currents are small compared with their sum, in most of the nodes. Hence the set (B18) can be considered as a perturbation series, the leading term being the unit representation. As many unknowns are to be determined in a node as the number of node-faces. Making use of the continuity of the partial currents at node-faces allows one to reduce the number of unknowns. It can be shown, by means of the character table of the considered group, that in slabs and regular triangles the unit representation determines the other irrep(s). It is shown below that in square nodes two irreps determine the others thus the number of unknowns is reduced to solely two, alike in Weiss' vectorial model [66].

Symmetry transformations of the square constitute the group C_{4v}. The character table of this group is given in Table B.1. The irreps of the incoming currents can be read out from the decomposition of the four component vector:

$$\begin{bmatrix} I_1^{(o)} \\ I_2^{(o)} \\ I_3^{(o)} \\ I_4^{(o)} \end{bmatrix} = \frac{I_1^{(o)}+I_2^{(o)}+I_3^{(o)}+I_4^{(o)}}{4} \begin{bmatrix} 1 \\ 1 \\ 1 \\ 1 \end{bmatrix} + \frac{I_1^{(o)}-I_2^{(o)}}{2} \begin{bmatrix} 1 \\ -1 \\ 0 \\ 0 \end{bmatrix} + \frac{I_3^{(o)}-I_4^{(o)}}{2} \begin{bmatrix} 0 \\ 0 \\ 1 \\ -1 \end{bmatrix} , \qquad (B19)$$

and the continuity condition is written as

$$I_\ell^{(o)} = \sum_{k=1}^{4} X_k^{(o)} c_{k\ell} = J_{\ell'}^{(\ell)} = \sum_{k=1}^{4} Y_k^{(\ell)} c_{k\ell'} = \sum_{k=1}^{4} Q_k^{(\ell)} X_k^{(\ell)} c_{k\ell'} , \qquad (B20)$$

$$J_\ell^{(\ell)} = \sum_{k=1}^{4} Y_k^{(\ell)} c_{k\ell} = \sum_{k=1}^{4} Q_k^{(\ell)} X_k^{(\ell)} c_{k\ell} = I_{\ell'}^{(\ell)} = \sum_{k=1}^{4} X_k^{(\ell)} c_{k\ell'} , \qquad (B21)$$

and the matrix $c_{k\ell}$ constructed from the column vectors in Eq.(B19). Each sum contains only three non-zero terms and the first (i.e. the unit) representation and the last representation occurs in each sum, therefore the other two irreps are determined if the first and last irreps are known in every node. The fourth irrep may be treated as a perturbation of the first one, and this circumstance considerably simplifies the numerical procedure.

The method presented can be compared to the vectorial model, where the iteration goes along the x and y axis, and the two improvements are almost the same in magnitude [66].

The nodal equations, equivalent to RME may promote the search for equivalent homogeneous diffusion parameters. A numerical method [102] was proposed by Laletin for determining the equivalent diffusion parameters. That method assumes that solutions in every node are well approximated by the sum of problems reflecting the node's most important characteristics, represented as responses. In simple cases that solution proves identical with the one presented here, though the FD equations are formulated there using the continuity of fluxes and currents along node-faces. Moreover the number of unknowns is not two, as here and in the vectorial model, but four.

ACKNOWLEDGEMENTS

The following subroutines were taken from the SIXTUS code, written by Dr. Jacek Arkuszewski: RASTER, CHART, MULTIN, XSECT, ALBEDO, MULTFL, MATRIX, EDITOR. The subroutine MI (matrix inversion) was written by Dr. Zoltan Szatmary. The author is indebted to Eidg. Institut für Reaktorforschung, Würenlingen, where a part of this method has been elaborated, and Dr. Jacek Arkuszewski's contribution to programming is acknowledged.

REFERENCES

[1] A. Weinberg, E. Wigner: The Physical Theory of Neutron Chain Reactors, Univ. of Chicago Press, Chicago (1980)

[2] R. Courant, D. Hilbert: Methods for Mathematical Physics, Vol.1., Interscience Publisher, New York (1962)

[3] L.D. Landau, E.M. Lifsitz: Theoretical Physics, Vol.V., Statistical Physics, Chapter 13, Pergamon Press, London (1959)

[4] S. Chandrasekar: Radiative Transfer, Dover, New York (1962)

[5] J.H. Ferziger, H.G. Kaper: Mathematical Theory of Transport Processes in Gases, North-Holland, Amsterdam (1972)

[6] N.A. Krall, A.W. Trivelpiece: Principles of Plasma Physics, McGraw Hill, New York (1973)

[7] M. Mitchner, C.H. Kruger: Partially Ionized Gases, John Wiley and Sons, New York (1973)

[8] The fields where transport theory is used is rather wide. See J.J. Duderstadt, W.R. Martin: Transport Theory, John Wiley and Sons, New York (1979) and the references at the end of the first chapter.

[9] A.F. Henry: Nuclear Reactor Analysis, MIT Press, Cambridge, Mass. (1975)

[10] Reactor Theory and Power Reactors, IAEA-SMR-44, ICTP, Trieste (1978)

[11] H. Greenspan et al.: Computing Methods in Reactor Physics, Atomizdat, Moscow (1972) in Russian

[12] A.F. Henry: Refinements in Accuracy of Coarse-Mesh Finite-Difference Solution of the Group Diffusion Equations, IAEA/SM-154/21, Seminar on Numerical Reactor Calculations, Vienna (1972)

[13] M.R. Wagner: Current Trends in Static Reactor Calculations, CONF-750413, Washington, 1, 1 (1975)

[14] J.J. Dorning: Modern Coarse-Mesh Methods - A Development of the '70's, In: Proc. Conf. on Computational Methods in Nuclear Engineering, Williamsburg, Vol.1., p. 3-1 (1979)

[15] G. Strang, G.J. Fix: An Analysis of the Finite Element Method, Prentice Hall, Englewood Cliffs (1979)

[16] O.C. Zienkiewicz: The Finite Element Method in Engineering Science, McGraw Hill, London (1971)

[17] D.M. Davierwalla: FINELM - A Multigroup Finite Element Code, Report EIR-419, Eidg. Institut für Reaktorforschung, Würenlingen (1980)

[18] Recent development in FEM is reported in several papers of the Proceedings of the International Topical Meeting on Advances in Mathematical Methods for the Solution of Nuclear Engineering Problems; to refer this conference the abbreviation ANS/ENS MTG, Munich (1981) will be used.

[19] F.C. Fayers, G. Nash: Annals of Nucl. Sci. Eng., 1, 185 (1974)

[20] W.B. Terney: Trans. Am. Nucl. Soc., 18, 319 (1974)

[21] S. Borresen: Nucl. Sci. Eng., 44, 37 (1971)

[22] S. Borresen: Trans. Am. Nucl. Soc., 15, 956 (1972)

[23] S. Borresen: Experience, Status and Advanced Application of PRESTO, Munich, ANS/ENS MTG, 1, 283 (1981)

[24] G. Aghte, S. Thomas: Program PYTHIA-4 - Physikalische Grundlagen, Report KKAB-75-75-O, KKAB, Berlin (1975)

[25] A.A. Marakazov: Calculation of Power Distribution in Two-Group Diffusion Theory, Report ИАЭ-2781, Kurchatov Inst., Moscow (1977) in Russian

[26] V. Krysl, M. Lehmann: BORORO - A New Fast 2D Diffusion Code for Pin Power Calculations with Modifiied Finite-Difference Approximation, In: Proc. of 7th Symposium of the Temporary International Collective for WWER Physics Study, Dobzhihovicze, Vol.2., p. 408 (1978) in Russian

[27] H. Sievers: Tagungsbericht der Reaktortagung 1974 des Deutschen Atomforums/KTG in Berlin, p. 60 (1974)

[28] H. Lukas, U. Wehmann: A Fast Two- and Three-Dimensional One-Group Coarse-Mesh Diffusion Program in Hexagonal Geometry, Munich, ANS/ENS MTG, 1, 299 (1981)

[29] A. Birkhofer, W. Werner: Efficiency of Various Methods for the Analysis of Space-Time Kinetics, CONF-730414, Washington, p. IX-31 (1973)

[30] A. Birkhofer et al.: Trans. Am. Nucl. Soc., 18, 153 (1974)

[31] J.A. Wooley: Three-Dimensional BWR Simulator, Report NEDO-20953, General Electric Co., San Jose (1976)

[32] S.G. Glasstone, E.D. Edlund: The Elements of Nuclear Reactor Theory, D. van Nostrand, Princetown, New Jersey, pp. 240-243 (1963)

[33] R. Avery: Theory of Coupled Reactors,
In: Proc. U. N. Intern. Conf. Peaceful Uses of Atomic Energy, 2nd, Geneve, Vol.12., p. 182 (1958)

[34] R.G. Rockwell, R.B. Perez: Kinetic Theory of Spatial and Spectral Coupling of the Reactor Neutron Field, CONF-650413-13, USAEC, p. 323 (1958)

[35] D.C. Wade, H.H. Rubin: Trans. Am. Nucl. Soc., 10, 250 (1967)

[36] M.G. Stevenson, S.J. Gage: J. Nucl. Energy, 24, 1 (1969)

[37] C.P. Robinson, R.R. Lee: Trans. Am. Nucl. Soc., 15, 297 (1972)

[38] T.G. Ober et al.: Nucl. Sci. Eng., 64, 605 (1977)

[39] C.P. Robinson, R.R. Lee: Trans. Am. Nucl. Soc., 17, 476 (1973)

[40] T.G. Ober et al.: Trans. Am. Nucl. Soc., 28, 763 (1978)

[41] T. Burns, J. Dorning: An Integral Balance Technique for Space- and Energy-Dependent Reactor Calculations, CONF-730414, Washington, Vol.II., p. VII-162 (1973)

[42] H. Finnemann et al.: Atomkernenergie, 30, 123 (1977)

[43] M.R. Wagner et al.: Atomkernenergie, 30, 129 (1977)

[44] C. Maeder: A Nodal Diffusion Method with Legendre Polynomials, CONF-780401, Williamsburg, p. 121 (1978)

[45] R.A. Shober: A Nodal Method for Solving Transient Few Group Neutron Diffusion Equation, Report ANL-78-51, Argonne Laboratory (1978)

[46] R.D. Lawrence, J.J. Dorning: Nucl. Sci. Eng., 76, 218 (1980)

[47] G. Greenman et al.: Recent Advances in an Analytic Nodal Method for Static and Transient Reactor Analysis,
In: ANS Conference on Computational Methods in Nuclear Engineering, Williamsburg, Virginia, Vol.1., p. 3-49 (1979)

[48] R.A. Shober: A Nodal Method for Fast Reactor Analysis, ibid, Vol.1., p. 3-33

[49] Z. Weiss: Nucl. Sci. Eng., 63, 457 (1977)

[50] E. Kaloinen et al.: Two Group Nodal Calculations in Hexagonal Fuel Assembly Geometry,
In: Proc. of Calculations of 3D Rating Distributions in Operating Reactors, Paris, p. 111 (1979)

[51] T. Duracz: A Nodal Method for Hexagonal Geometry, Munich, ANS/ENS MTG, 1, 423 (1981)

[52] K. Aoki, M. Tsuiki: Nucl. Sci. Eng., 57, 53 (1975)

[53] J. Arkuszewski: SIXTUS a Two-Dimensional Diffusion Theory Nodal Code in Hexagonal Geometry, Report EIR-410, Eidg. Institut für Reaktorforschung, Würenlingen (1980)

[54] C. de Boor, B. Swartz: Siam J. of Numer. Anal., 10, 57 (1973)

[55] R.A. Shober et al.: Nucl. Sci. Eng., 64, 582 (1977)

[56] M. Makai, C. Maeder: Trans. Am. Nucl. Soc., 35, 237 (1980)

[57] R.A. Shober: Trans. Am. Nucl. Soc., 28, 249 (1978)

[58] CETRA is a modified version of the COMETA code, see G.P. Bottoni: Trans. Am. Nucl. Soc., 28, 251 (1978); R. Bonalumi et al.: Trans. Am. Nucl. Soc., 20, 362 (1975)

[59] R. Bonalumi et al.: MUSIC a Mesh-Unrestricted Simulation Code, CONF-780401, Gattlinburg, p. 169 (1978)

[60] M. Melice: A Nodal-Modal Coarse-Mesh Method, Report NEACRP-L-228, Electrobel, Brussels (1978)

[61] M. Makai: Symmetries and the Coarse-Mesh Method, Report EIR-414, Eidg. Institut für Reaktorforschung, Würenlingen (1980)

[62] R.G. Steinke: Trans. Am. Nucl. Soc., 17, 230 (1973)

[63] H.W. Graves, Jr.: The Evaluation of Power Distribution in Large Reactors Using a Two-Group Nodal Method, Ph. D. Thesis, Univ. of Michigan, Ann. Arbor. (1973)

[64] T.J. Burns, J.J. Dorning: Trans. Am. Nucl. Soc., 19, 174 (1974)

[65] J.J. Dorning: A Review of Green's Function Methods in Computational Fluid Mechanics, Munich, ANS/ENS MTG, 1, 437 (1981)

[66] Z. Weiss: Nucl. Sci. Eng., 48, 235 (1972)

[67] Z. Weiss: Trans. Am. Nucl. Soc., 23, 198 (1976)

[68] J.B. Yasinsky, S. Kaplan: Nucl. Sci. Eng., 28, 426 (1967)

[69] J.W. Riese: Trans. Am. Nucl. Soc., 7, 22 (1964)

[70] D.L. Delp et al.: FLARE - A 3D BWR Simulator, GEAP-4598, General Electric Company, San Jose (1964)

[71] L. Goldstein et al.: Trans. Am. Nucl. Soc., 10, 300 (1967)

[72] P. Lindrgen et al.: POLCA - A 3D BWR Simulator, in Trans. Reaktortagung Deutsches Atomforum E.V., Paper 110 (1971)

[73] H.L. Dodds et al.: Trans. Am. Nucl. Soc., 14, 212 (1971)

[74] A. Amouyal et al.: J. Nucl. Energy, 6, 79 (1957)

[75] V.V. Orlov: Albedo in Diffusion and Slowing-Down Theory
In: Reactor Physics (Ed.: P.A. Krupniczky) Gostatomizdat, Moscow, pp. 177-191 (1961) in Russian

[76] A. Muller, M.R. Wagner: Trans. Am. Nucl. Soc., 15, 280 (1972); Recent applications are given in N.K. Gupta: Atomkernenergie, 38, 194 (1981)

[77] D.M. Verplanck, D.R. Fergusson: SIMULATE Reactor Simulation Code, Yankee Atomic Energy Company, Boston (1972)

[78] A. Ancona: Reactor Nodal Methods Using Response Matrix Techniques, Ph. D. Thesis, Rensselaer Polytechnic Institute (1977)

[79] D.R. Harris: ANDIMG3, the Basic Program of a Series of Monte-Carlo Programs, LA-4539, Los Alamos (1970)

[80] K. Koebke, M.R. Wagner: Atomkernenergie, 30, 136 (1977)

[81] R. Fröhlich: Atomkernenergie, 30, 152 (1977)

[82] K. Koebke: Advances in Homogenization and Dehomogenization, Munich, ANS/ENS MTG, 2, 59 (1981)

[83] IMSL Reference Manual, IMSL Public Service, Houston, Vol.2., p. E-1 (1980)

[84] B.T. Smith et al.: Matrix Eigensystem Routins -EISPACK Guide, Lecture Notes in Computer Science, Springer Publ., Berlin, Vol.6., pp. 41-48 (1976)

[85] M. Makai, J. Arkuszewski: Trans. Am. Nucl. Soc., 38, 347 (1981)

[86] D.R. Vondy, T.B. Fowler: Nucl. Sci. Eng., 65, 415 (1978)

[87] M.R. Wagner: GAUGE - A 2D Few-Group Neutron Diffusion Depletion Program for a Uniform Triangular Mesh, Report GA-8307, General Atomics, San Diego (1968)

[88] R. Ruhle: RSYST - An Integrated Modular System with Data Basis for Automated Calculation of Nuclear Reactors, Report ORNL-TR-2796, Oak Ridge National Laboratory, Oak Ridge (1973)

[89] Benchmark Problem Book, ANL-7416, Suppl.2., Argonne National Laboratory (1977)

[90] R. Steinke: Personal Communication (1981)

[91] W.R. Davison: BUG180/HTGR - A 2D Triangular Mesh Multigroup Diffusion Burnup Code for Use in the Design of 180° Rotationally Symmetric HTGR Cores, Report GA-A12674, General Atomics, San Diego (1975)

[92] S. Lie: Vorlesungen über Differential Gleichnungen, Teubner, Leipzig (1981)

[93] L.V. Ovsjannikov: Group Analysis of Differential Equations, Nauka, Moscow (1978) in Russian

[94] F. Gonsales-Gasgon: J. Math. Phys., 18, 1763 (1977)

[95] F. Gonsales-Gasgon: J. Math. Phys., 21, 2046 (1977)

[96] B.G. Konopelchenko, V.G. Mokhnachev: J. Phys. A: Math. Gen., 13, 3113 (1980)

[97] L.M. Falicov: Group Theory and its Applications, The Univ. of Chicago Press, Chicago (1966)

[98] L.D. Landau, E.M. Lifsitz: Theoretical Physics, Quantum Mechanics, Chapter 12, Vol.III., Pergamon Press, London (1959)

[99] M. Goldsmith: Nucl. Sci. Eng., 17, 111 (1963)

[100] S.O. Lindahl, Z. Weiss: The Response Matrix Method, In: Advances in Nuclear Science and Technology, Plenum Press, New York, Vol.13., p. 73 (1981)

[101] P. Mohanakrishnan: Progr. in Nucl. Energy, 7, 1 (1981)

[102] N.I. Laletin, A.V. Elshin: Derivation of Finite-Difference Equations for Heterogeneous Reactor, Report НАЭ-3280/5, Kurchatov Institute, Moscow (1980) in Russian

TABLES

Table 6.1 Boundary condition in HEXAN

Boundary condition index	Determination of incoming current
1	I=0 (vacuum)
2	I=J (reflection)
3	I=α·J (albedo)
4-9	180 degree symmetry in the node
4	I6=I1 , I5=I2 , I4=I3
5	I1=I2 , I6=I3 , I5=I4
6	I1=I4 , I2=I3 , I6=I5
7	I1=I6 , I2=I5 , I3=I4
8	I2=I1 , I3=I6 , I4=I5
9	I3=I2 , I4=I1 , I5=I6
10-15	60 degree rotational symmetry
10	I_I=I1 , I≠1
11	I_I=I2 , I≠2
12	I_I=I3 , I≠3
13	I_I=I4 , I≠4
14	I_I=I5 , I≠5
15	I_I=I6 , I≠6
16	rotational symmetry, upper edge I2, I3 and I4 are to be determined from outcurrents of lower edge of the core
17	rotational symmetry, lower edge I4, I5 and I6 are to be determined from outcurrents of upper edge of the core

Table 7.1 Benchmark problem results for Marakazov's benchmark

Program	k_{eff}	ΔP* (%)	Ref.
TRIGON	0.97756	<1	[25]
BIPR-6	0.97804	0.8	[25]
KR-3	0.97760	0.2	[25]
KR-4	0.97760	0.0	[25]
M2	0.97734	2.5	[51]
M3	0.97734	1.7	[51]
SIXTUS	0.97576	1.4	[53]
HEXAN	0.97805	1.6	-
ΔP - maximum error in power density (%)			

Table 7.2a

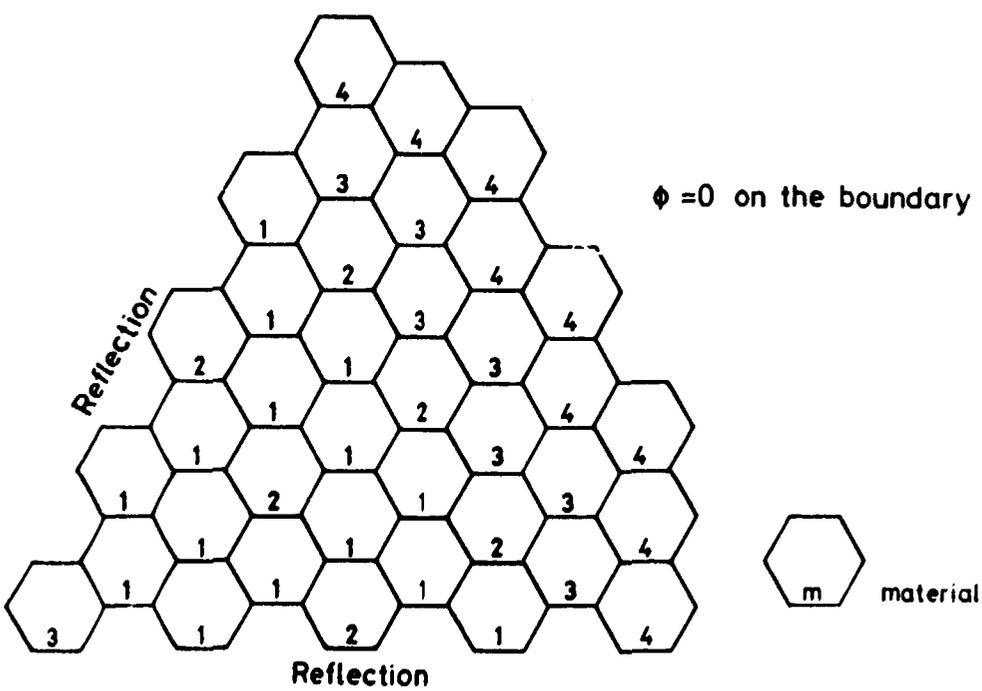

Table 7.2b The WWER-1000 benchmark specification

	$\Sigma_{(i-1)\to i}$	D_i	Σ_{ai}	Σ_{fi}	$\nu\Sigma_{fi}$	$\Sigma_{rem,i}$
Material No1		χ = (0.76, 0.24, 0, 0)				
1	0	2.1309	3.421×10^{-3}	7.2825×10^{-3}	7.2825×10^{-3}	7.8908×10^{-2}
2	7.5487×10^{-2}	0.91964	2.248×10^{-3}	5.7354×10^{-4}	5.7354×10^{-4}	9.1544×10^{-2}
3	8.9296×10^{-2}	0.65946	2.1423×10^{-2}	8.0392×10^{-3}	8.0392×10^{-3}	9.6368×10^{-2}
4	7.4945×10^{-2}	0.19274	8.3783×10^{-2}	0.10807	1.0807×10^{-1}	8.3783×10^{-2}
Material No2		χ = (0.76, 0.24, 0, 0)				
1	0	2.1318	3.4810×10^{-3}	7.4381×10^{-3}	7.4381×10^{-3}	7.8946×10^{-2}
2	7.5465×10^{-2}	0.91964	2.378×10^{-3}	8.6043×10^{-4}	8.6043×10^{-4}	9.1541×10^{-2}
3	8.9163×10^{-2}	0.6563	2.359×10^{-2}	1.1877×10^{-2}	1.1877×10^{-2}	9.7569×10^{-2}
4	7.3980×10^{-2}	0.1912	1.0186×10^{-1}	0.1473	1.473×10^{-1}	1.0186×10^{-1}
Material No3		χ = (0.76, 0.24, 0, 0)				
1	0	2.1318	3.498×10^{-3}	7.4846×10^{-3}	7.485×10^{-3}	7.8955×10^{-2}
2	7.5457×10^{-2}	0.91964	2.422×10^{-3}	9.4609×10^{-4}	9.461×10^{-4}	9.1543×10^{-2}
3	8.9121×10^{-2}	0.6554	2.4257×10^{-2}	1.3012×10^{-2}	1.301×10^{-2}	9.7953×10^{-2}
4	7.3696×10^{-2}	0.19065	1.0679×10^{-1}	0.1578	0.1578	0.10679
Material No4		χ = (0, 0, 0, 0)				
1	0	2.4600	4.5×10^{-4}	0.0	0.0	0.1082
2	0.10775	0.8987	0.0	0.0	0.0	0.1559
3	0.1559	0.5896	1.0×10^{-3}	0.0	0.0	0.1277
4	0.1267	0.1393	1.677×10^{-2}	0.0	0.0	0.1677

Table 7.3 The influence of the overrelaxation weight on the convergence for WWER-1000 benchmark

k_{eff}	Δk_{eff}	$\Delta\phi$	ITO	ITI	TIME (sec)	WEIGHT
-	-	-	-	-	>180	-0.005
1.11207	0.3	8	26	3	163.6	0.0
-	-	-	-	3	>180	0.05
1.11209	0.3	9	26	2	128.6	0.4
1.11206	0.3	9	29	2	150.6	0.3
1.11206	<0.01	8	32	2	150.3	0.2
non-convergent				2		0.1
1.11208	<0.01	1	25	2	120.0	0.0
non-convergent				2		-0.1
non-convergent				2		-0.2
non-convergent				2		-0.3

Table 7.4 Results for the GA9A1 HTGR benchmark problem

Program	k_{eff}	PTS/NODE	P (%)	$\Delta\phi$	Time (sec)	Machine	Ref.
BUG180	1.11815	48	0.0	10^{-5}	9660	UNIVAC 1108	[91]
GRIMHX	1.12028	6	5.1	10^{-5}	26	IBM S-360/195	[89]
GRIMHX	1.11863	6	3.1	10^{-5}	10	IBM S-360/195	[89]
VENTURE	1.11860	54	-	10^{-5}	171.6	IBM 360/195	[90]
VENTURE	1.12725	1	-	10^{-5}	36.6	IBM 360/195	[90]
DIFGEN	1.0913	6	-	10^{-5}	500	CYBER 174	[90]
DIFGEN	1.0916	6	-	10^{-5}	270	CYBER 174	[90]
VALE	1.11814	48	-	10^{-5}	154	IBM 360/91	[90]
VALE	1.11671	3	-	10^{-5}	18	IBM 360/91	[90]
SIXTUS*	1.11650	1	2.4	5×10^{-5}	96.9	EC-1040	-
HEXAN	1.11888	1	1.5	3×10^{-5}	537.3	EC-1040	-

*An IBM adapted version.

1 sec IBM 360/195 ≈ 2 sec IBM 360/91 ≈ 4 sec CYBER 174 ≳ (11 sec UNIVAC 1108) ≈ 30 sec EC-1040

Table 7.5 Impact of weight in overrelaxation on the convergence

k_{eff}	$\Delta\phi$ ($\times 10^{-5}$)	ITI	WEIGHT	TIME (sec)
1.11888	0.2	3	0.0	515
1.11873	80	3	0.1	302
1.11863	60	3	0.2	611
1.11887	3	5	0.0	635

Table A.1 Elements of the group C_{6v}

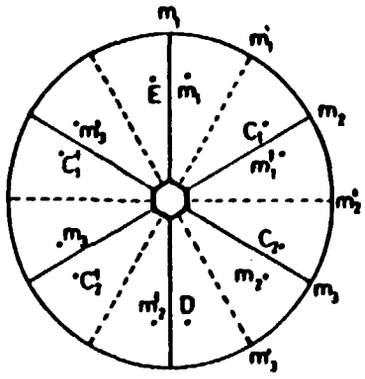

identity operation		$\equiv E$
rotation by $\pi/3$		$\equiv C_1$
rotation by $2\pi/3$		$\equiv C_2$
rotation by		$\equiv D$
rotation by $-2\pi/3$		$\equiv C_2^{-1}$
rotation by $-\pi/3$		$\equiv C_1^{-1}$
reflection through m_1	plane	$\equiv m_1$
m_2		$\equiv m_2$
m_3		$\equiv m_3$
reflection through m_1'	plane	$\equiv m_1'$
m_2'		$\equiv m_2'$
m_3'		$\equiv m_3'$

Table B.1 Character table of the group C_{4v}

Repr./Class	C	$2C_a$	$2C_d$	C_b	$2C_c$
Γ_1	1	1	1	1	1
Γ_2	1	-1	-1	1	1
Γ_3	1	1	-1	1	-1
Γ_4	1	-1	1	1	-1
Γ_5	2	0	0	-2	0

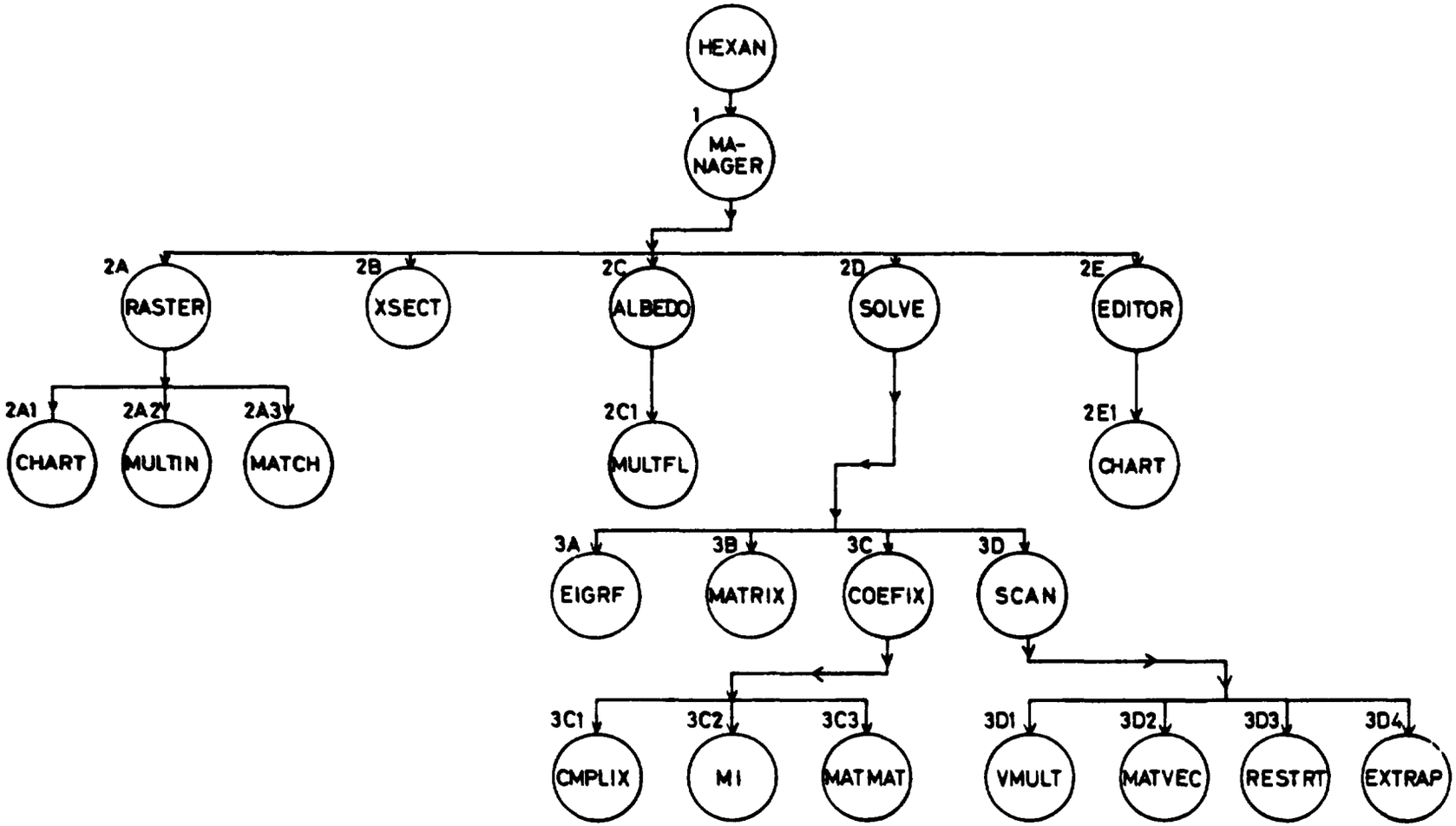

Fig. 5.1 Flow-chart of HEXAN

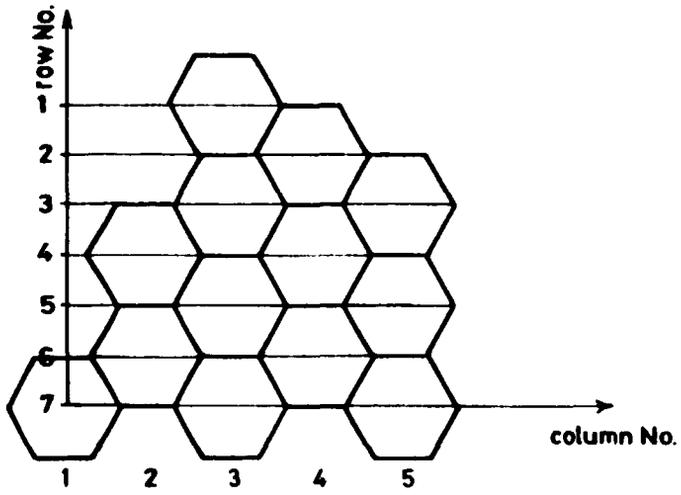

Fig. 6.1 *Map of nodes for HEXAN*

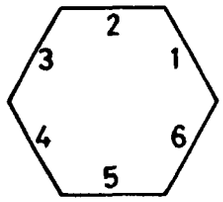

Fig. 6.2 *Numbering of nodes faces*

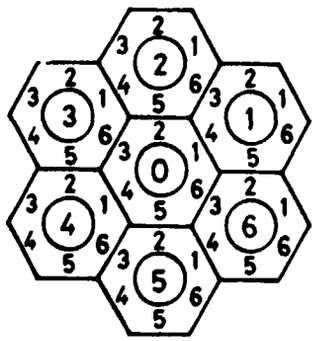

Fig. B.1 *The node and face numbering*

Kiadja a Központi Fizikai Kutató Intézet
Felelős kiadó: Gyimesi Zoltán
Szakmai lektor: Gadó János
Nyelvi lektor: Szabó Zoltán
Gépelte: Polgár Julianna
Példányszám: 315 Törzsszám: 82-379
Készült a KFKI sokszorosító üzemében
Felelős vezető: Nagy Károly
Budapest, 1982. július hó